

**High Transverse Momentum Physics at the Large Hadron Collider ***

The U.S. ATLAS and U.S. CMS Collaborations

edited by

Ian Hinchliffe

E.O. Lawrence Berkeley National Laboratory, Berkeley, CA 94720

John Womersley

*Fermi National Accelerator Laboratory, Batavia, IL 60510***ABSTRACT**

This note summarizes the various physics studies done for the LHC. It concentrates on the processes involving the production of high mass states. Results are drawn from simulations performed by the CMS and ATLAS collaborations. The ability of the LHC to provide insight into the mechanism of electroweak symmetry breaking is exemplified.

I. Introduction and Motivation

This document is intended to summarize the potential of the Large Hadron Collider (LHC) for high transverse momentum physics and explain the reasons why it is a crucial next step in our understanding of the behavior of nature. It is the physics potential of the LHC that motivates US participation; not a desire to build detector components, a need for projects for students or postdocs, or a requirement for a future program to retain university funding (though these elements may be important). We believe this physics potential enormous and that, among currently approved projects, the LHC is unique in that it is the only one that has sufficient energy and luminosity to probe in detail the energy scale relevant to electroweak symmetry breaking.

We outline the many physics processes that have been studied as part of the design processes for the ATLAS[1] and CMS[2] detectors. Examples are selected from the large amount of detailed work carried out for and since the technical proposals.

A. The Standard Model

The Standard Model (SM) is a very successful description of the interactions of the components of matter at the smallest scales ($\lesssim 10^{-18}$ m) and highest energies (~ 200 GeV) accessible to current experiments. It is a quantum field theory which describes the interaction of spin- $\frac{1}{2}$, point-like fermions, whose interactions are mediated by spin-1 gauge bosons. The bosons are a consequence of local gauge invariance applied to the fermion fields and are a manifestation of the symmetry group of the theory, which for the SM is $SU(3) \times SU(2) \times U(1)$.

The fundamental fermions are leptons and quarks. The left-handed states are doublets under the $SU(2)$ group, while the right-handed states are singlets. There are three generations of

fermions, each generation identical except for mass: the origin of this structure, and the breaking of generational symmetry (flavor symmetry) remain a mystery. There are three leptons with electric charge -1 , the electron (e), muon (μ) and tau lepton (τ), and three electrically neutral leptons (the neutrinos ν_e , ν_μ and ν_τ). Similarly there are three quarks with electric charge $+\frac{2}{3}$, up (u), charm (c) and top (t), and three with electric charge $-\frac{1}{3}$, down (d), strange (s) and bottom (b). The quarks are triplets under the $SU(3)$ group and thus carry an additional “charge,” referred to as color. There is mixing between the three generations of quarks, which in the SM is parameterized by the Cabibbo-Kobayashi-Maskawa (CKM)[3] matrix but not explained.

In the SM the $SU(2) \times U(1)$ symmetry group (which describes the so-called Electroweak interaction) is spontaneously broken by the existence of a (postulated) Higgs field with non-zero expectation value. This leads to the emergence of massive vector bosons, the W^\pm and Z , which mediate the weak interaction, while the photon of electromagnetism remains massless. One physical degree of freedom remains in the Higgs sector, which should be manifest as a neutral scalar boson H^0 , but which is presently unobserved. The $SU(3)$ group describes the strong interaction (quantum chromodynamics or QCD). Eight vector gluons mediate this interaction. They carry color charges themselves, and are thus self-interacting. This implies that the QCD coupling α_S is small for large momentum transfers but large for small momentum transfers, and leads to the confinement of quarks inside color-neutral hadrons. Attempting to free a quark produces a jet of hadrons through quark-antiquark pair production and gluon bremsstrahlung.

The basic elements of the Standard Model were proposed in the 1960’s and 1970’s [6]. Increasing experimental evidence of the correctness of the model accumulated through 1970’s and 1980’s:

- SLAC deep inelastic scattering experiments showed the existence of point-like scattering centers inside nucleons, later identified with quarks [7]
- observation of the c and b quarks [8]
- observation of neutral weak currents (Z exchange)[9]
- observation of jet structure and three-jet final states (gluon radiation) in e^+e^- and hadron-hadron collisions[10]

* To appear in the Proceedings of the 1996 DPF/DPB Summer Study on New Directions for High Energy Physics (Snowmass 96).

- direct observation of the W and Z at the CERN SPS collider [12]

Following these discoveries, an era of consolidation has been entered. Ever more precise experiments have been carried out at LEP and SLC which have provided verification of the couplings of quarks and leptons to the gauge bosons at the level of 1-loop radiative corrections ($\sim \mathcal{O}(10^{-3})$). The top quark was discovered at Fermilab in 1995, with a very large mass (~ 175 GeV).[11]

Only two particles from the Standard Model have yet to be observed; ν_τ and the Higgs boson. Of these the latter is more important as it holds the key to the generation of W , Z , quark and lepton masses. Some of the SM parameters, particularly those of the CKM matrix are not well determined. Experiments over the next few years involving CP violation in the K[4] and B systems[5] should determine these parameters or demonstrate the SM cannot adequately explain CP violation. There are some indications that the SM may be incomplete or inadequate in that there are a very few experimental observations that it cannot accommodate such as the possibility that neutrino oscillations occur[13].

B. Beyond the Standard Model

The success of the standard model[6] of strong (QCD), weak and electromagnetic interactions has drawn increased attention to its limitations. In its simplest version, the model has 19 parameters [14], the three coupling constants of the gauge theory $SU(3) \times SU(2) \times U(1)$, three lepton and six quark masses, the mass of the Z boson which sets the scale of weak interactions, the four parameters which describe the rotation from the weak to the mass eigenstates of the charge -1/3 quarks (CKM matrix). All of these parameters are determined with varying errors. Of the two remaining, one, a CP violating parameter associated with the strong interactions, must be very small. The last parameter is associated with the mechanism responsible for the breakdown the electroweak $SU(2) \times U(1)$ to $U(1)_{em}$. This can be taken as the mass of the, as yet undiscovered, Higgs boson. The couplings of the Higgs boson are determined once its mass is given.

The gauge theory part of the SM has been well tested; but there is no direct evidence either for or against the simple Higgs mechanism for electroweak symmetry breaking. All masses are tied to the mass scale of the Higgs sector. Within the model we have no guidance on the expected mass of the Higgs boson. The current experimental lower bound is 65 GeV. As its mass increases, the self couplings and the couplings to the W and Z bosons grow[15]. This feature has a very important consequence. Either the Higgs boson must have a mass less than about 800 GeV or the dynamics of WW and ZZ interactions with center of mass energies of order 1 TeV will reveal new structure. It is this simple argument that sets the energy scale that must be reached to guarantee that an experiment will be able to provide information on the nature of electroweak symmetry breaking.

The presence of a single elementary scalar boson is distasteful to many theorists. If the theory is part of some more fun-

damental theory, which has some other larger mass scale (such as the scale of grand unification or the Planck scale), there is a serious “fine tuning” or naturalness problem. Radiative corrections to the Higgs boson mass result in a value that is driven to the larger scale unless some delicate cancellation is engineered ($m_0^2 - m_1^2 \sim M_W^2$ where m_0 and m_1 are order 10^{15} GeV or larger). There are two ways out of this problem which involve new physics on the scale of 1 TeV. New strong dynamics could enter that provide the scale of m_W or new particles could appear so that the larger scale is still possible, but the divergences are cancelled on a much smaller scale. In any of the options, standard model, new dynamics or cancellations, the energy scale is the same; something must be discovered on the TeV scale.

Supersymmetry is an appealing concept for which there is, at present, no experimental evidence[16]. It offers the only presently known mechanism for incorporating gravity into the quantum theory of particle interactions and provides an elegant cancellation mechanism for the divergences provided that at the electroweak scale the theory is supersymmetric. The successes if the Standard Model (such as precision electroweak predictions) are retained, while avoiding any fine tuning of the Higgs mass. Some supersymmetric models allow for the unification of gauge couplings at a high scale and a consequent reduction of the number of arbitrary parameters. Supersymmetric models postulate the existence of superpartners for all the presently observed particles: bosonic superpartners of fermions (squarks \tilde{q} and sleptons $\tilde{\ell}$), and fermionic superpartners of bosons (gluinos \tilde{g} and gauginos $\tilde{\chi}_i^0, \tilde{\chi}_i^\pm$). There are also multiple Higgs bosons: h, H, A and H^\pm . There is thus a large spectrum of presently unobserved particles, whose exact masses, couplings and decay chains are calculable in the theory given certain parameters. Unfortunately these parameters are unknown. Nonetheless, if supersymmetry is to have anything to do with electroweak symmetry breaking, the masses should be in the region 100 GeV – 1 TeV.

An example of the strong coupling this scenario is “technicolor” or models based on dynamical symmetry breaking[17]. Again, if the dynamics is to have anything to do with Electroweak Symmetry breaking we would expect new states in the region 100 GeV – 1 TeV; most models predict a large spectrum. An elegant implementation of this appealing idea is lacking. However, all models predict structure in the WW scattering amplitude at around 1 TeV center of mass energy.

There are also other possibilities for new physics that are not necessarily related to the scale of electroweak symmetry breaking. There could be new neutral or charged gauge bosons with mass larger than the Z and W ; there could be new quarks, charged leptons or massive neutrinos; or quarks and leptons could turn out not to be elementary objects. While we have no definitive expectations for the masses of these objects, the LHC must be able to search for them over its available energy range.

C. Accelerator Facilities

High energy physics is explored experimentally by accelerating and colliding beams of quarks and leptons. Electrons

(and/or positrons) and protons (and/or antiprotons) are used in practice. It is much easier to reach high energies using protons, but each of the constituent quarks and gluons carries only a fraction of the total energy.

The present comprehensive state of understanding the Standard Model stems in large part from our having a wide range of facilities which explore the interactions between the fermions at energy scales \sqrt{s} of order $m_{W,Z} \sim 100$ GeV to $m_t \sim 180$ GeV. These are:

- The Fermilab Tevatron collider, with $p\bar{p}$ collisions at $\sqrt{s} = 1.8$ TeV;
- The CERN LEP collider, with e^+e^- collisions at $\sqrt{s} = m_Z$, increasing to about 180 GeV in LEP 2 (1996);
- The SLAC SLC collider, with e^+e^- collisions at $\sqrt{s} = m_Z$;
- The DESY HERA collider, which collides 30 GeV e^\pm with 800 GeV protons.

While either LEP 2 or the Tevatron may be sufficiently lucky to discover new physics in the coming decade, there is *only one* facility under construction that will really enable us to address interactions at energy scales 250 GeV – 1 TeV: CERN’s Large Hadron Collider. At present, this is our only sure window on to physics beyond the Standard Model.

II. The Large Hadron Collider

A. Machine parameters

The LHC machine is a proton-proton collider that will be installed in the 26.6 km circumference tunnel currently used by the LEP electron-positron collider at CERN [18]. The 8.4 tesla dipole magnets each 14.2 meters long (magnetic length) are of the “2 in 1” type; the apertures for both beams have common mechanical structure and cryostat. These superconducting magnets operate at 1.9K and have an aperture of 56 mm. They will be placed on the floor in the LEP ring after removal and storage of LEP. The 1104 dipoles and 736 quadrupoles support beams of 7 TeV energy and a circulating current of 0.54 A.

Bunches of protons separated by 25 ns and with an RMS length of 75 mm intersect at four points where experiments are placed. Two of these are high luminosity regions and house the ATLAS and CMS detectors. Two other regions house the ALICE detector [19], to be used for the study of heavy ion collisions, and LHC-B[20], a detector optimised for the study of B-mesons and B-Baryons. The beams cross at an angle of $200\mu\text{rad}$ resulting in peak luminosity of $10^{34} \text{ cm}^{-2} \text{ sec}^{-1}$ which has a lifetime of 10 hours. At the peak luminosity there are an average of $\sim 20pp$ interactions per bunch crossing. Ultimately, the peak luminosity may increase to $2 \times 10^{34} \text{ cm}^{-2} \text{ sec}^{-1}$. The machine will also be able to accelerate heavy ions resulting in the possibility of Pb-Pb collisions at 1150 TeV in the center of mass and luminosity up to $10^{27} \text{ cm}^{-2} \text{ sec}^{-1}$.

In the pp version, which will be the focus of the rest of this article, the LHC can be thought of as a parton-parton collider with beams of partons of indefinite energy. The effective

luminosity[21] of these collisions is proportional to the pp luminosity and falls rapidly with the center of mass energy of the parton-parton system. The combination of the higher energy and luminosity of the LHC compared to the highest energy collider currently operating, the Tevatron, implies that the accessible energy range is extended by approximately a factor of ten.

B. Physics Goals

The fundamental goal is to uncover and explore the physics behind electroweak symmetry breaking. This involves the following specific challenges:

- Discover or exclude the Standard Model Higgs and/or the multiple Higgses of supersymmetry.
- Discover or exclude supersymmetry over the entire theoretically allowed mass range.
- Discover or exclude new dynamics at the electroweak scale

The energy range opened up by the LHC gives us the opportunity to search for other, possibly less well motivated, objects:

- Discover or exclude any new electroweak gauge bosons with masses below several TeV.
- Discover or exclude any new quarks or leptons that are kinematically accessible.

Finally we have the possibility of exploiting the enormous production rates for certain standard model particles to conduct the following studies:

- The decay properties of the top quark, limits on exotic decays such as $t \rightarrow cZ$ or $t \rightarrow bH^+$.
- b -physics, particularly that of B-baryons and B_s mesons.

An LHC experiment must have the ability to find the unexpected. New phenomena of whatever type will decay into the particles of the standard model. In order to cover the lists given above a detector must have great flexibility. The varied physics signatures for these processes require the ability to reconstruct and measure final states involving the following

- Charged leptons including the tau.
- The electroweak gauge bosons W, Z and γ .
- Jets coming from the production at high transverse momentum of quarks and gluons.
- Jets that have b-quarks within them.
- (Missing transverse) Energy carried off by weakly interacting neutral particles such as neutrinos.

Particle ID which is required for a detailed study of b -physics, as opposed to b -tagging, is not part of ATLAS or CMS.

In the discussion of physics signals that we present below, it is necessary to estimate production cross sections for both signal and background processes. These are estimated using perturbative QCD and depend on several ingredients. Differences can arise from the structure functions that are used; the energy (Q^2 scale) used in the evaluation of the QCD coupling constant and the structure functions; and the order in QCD perturbation theory that is used in the calculation of the underlying parton process. These issues can make comparison between different simulations of the same process difficult. Higher order corrections are not known for all processes and in some cases they are known for the signal and not for the background. When the corrections are known, they are often not incorporated in the event generator tools that are employed. Except where noted, we have adopted a conservative approach and use calculations that are only to lowest order. Almost all higher order corrections increase the rates, and are sometimes included by multiplying the lowest order rates by a so-called K-factor. These corrections are typically ~ 1.5 and can occasionally be as large as 2.0. Since the corrections depend on kinematical details this procedure is at best an approximation. Uncertainties from the choice of scale and structure functions are at the 20% level except in cases involving the production of very light states. The total cross-section for b-quark production is particularly uncertain.

The level of simulation used in the processes varies quite widely. For a few processes a full GEANT[22] style simulation has been carried out. Such simulations are very slow ($\sim \text{few} \times 10^5$ Mips/event) and are difficult to carry out for processes where large number of events need to be simulated and many strategies for extracting signals need to be pursued. In these cases a particle level simulation and parameterized detector response is used. A lower level of simulation involving partons (*i.e.* leptons and jets) and parameterized response is fast and might be required when the underlying parton process is not present in full event generators. This last level of simulation is useful for exploring signals but often leads to overly optimistic results, particularly where the reconstruction of invariant masses of jets are involved. None of the results included here use this last level of simulation, unless stated explicitly.

C. Detectors

Two large, general-purpose pp collider detectors will be constructed for LHC: ATLAS[1] and CMS[2]. Both collaborations completed Technical Proposals for their detectors in December 1994, and were formally approved in January 1996. Though they differ in most details, the detectors share many common emphases which derive from the physics goals of LHC:

- they both include precision electromagnetic calorimetry;
- they both use a rather ambitious magnet (though of different geometries) in order to obtain good muon identification and precision momentum measurement;
- both have lepton identification and measurement over $|\eta| < 3$;

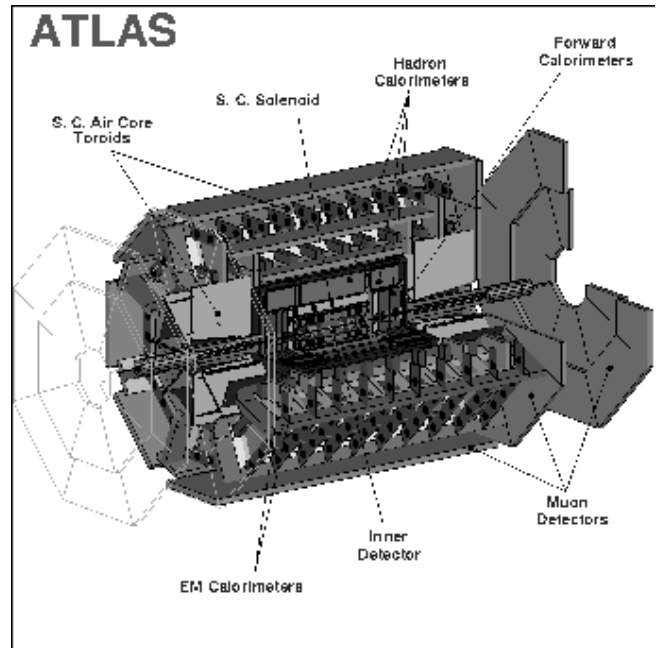


Figure 1: The ATLAS detector

- they both incorporate ambitious multi-layer silicon tracker systems for heavy flavor tagging (the usefulness of this capability is an important lesson from the Tevatron);
- they both include forward calorimetry for large η coverage in order to obtain the required \cancel{E}_T resolution.

The ATLAS detector is shown in Fig.1. It uses a tracking system employing silicon pixels, silicon strip detectors, and a transition radiation tracker, all contained within a superconducting solenoid. The charged track resolution is $\Delta p_T/p_T = 20\%$ at $p_T = 500$ GeV/c. The tracker is surrounded by an electromagnetic calorimeter using a lead-liquid argon accordion design; the EM calorimeter covers $|\eta| < 3$ (with trigger coverage of $|\eta| < 2.5$) and has a resolution of $\Delta E/E = 10\%/\sqrt{E} \oplus 0.7\%$. The hadronic calorimeter uses scintillator tiles in the barrel, and liquid argon in the endcaps ($|\eta| > 1.5$); its resolution is $\Delta E/E = 50\%\sqrt{E} \oplus 3\%$. Forward calorimeters cover the region $3 < |\eta| < 5$ with a resolution $\Delta E/E = 100\%\sqrt{E} \oplus 10\%$. Surrounding the calorimeters is the muon system. Muon trajectories are measured using three layers of chambers (MDT's and CSC's) in a spectrometer using a large air-core toroid magnet. The resulting muon momentum measurement is $\Delta p_T/p_T = 8\%$ at $p_T = 1$ TeV/c and $\Delta p_T/p_T = 2\%$ at $p_T = 100$ GeV/c. Muons may be triggered on over the range $|\eta| < 2.2$.

The CMS detector is shown in Fig.2. The tracking system is based on silicon pixels, silicon strip detectors, and microstrip gas chambers. The charged track resolution is $\Delta p_T/p_T = 5\%$ at $p_T = 1$ TeV/c and $\Delta p_T/p_T = 1\%$ at $p_T = 100$ GeV/c. CMS has chosen a precision electromagnetic calorimeter using lead tungstate (PbWO_4) crystals, covering $|\eta| < 3$ (with trigger coverage of $|\eta| < 2.6$). Its resolution at low luminosity is

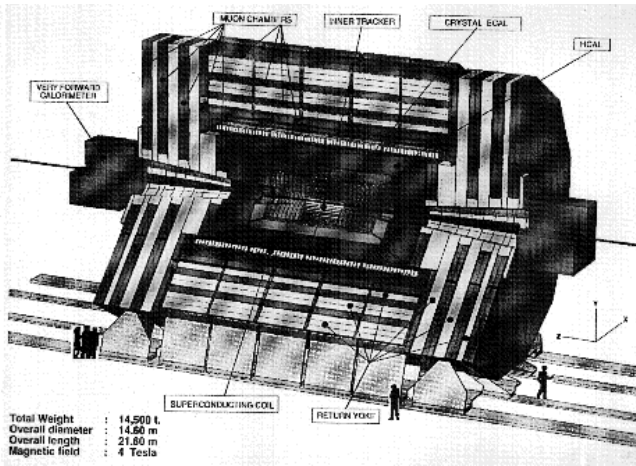


Figure 2: The CMS detector

$\Delta E/E = 2\% \sqrt{E} \oplus 0.5\%$. The surrounding hadronic calorimeter uses scintillator tiles in the barrel and endcaps; its resolution is $\Delta E/E = 65\% \sqrt{E} \oplus 5\%$. The region $3 < |\eta| < 5$ is covered by forward calorimeters using parallel-plate chambers or quartz fibers and having a resolution of about $\Delta E/E = 130\% \sqrt{E} \oplus 10\%$. The calorimeters are contained in a 4 tesla superconducting coil which provides the magnetic field for charged particle tracking. Muon trajectories outside the coil are measured in four layers of chambers (drift tubes and CSC's) embedded in the iron return yoke. The muon momentum measurement using the muon chambers and the central tracker covers the range $|\eta| < 2.4$ with a resolution $\Delta p_T/p_T = 5\%$ at $p_T = 1 \text{ TeV}/c$ and $\Delta p_T/p_T = 1\%$ at $p_T = 100 \text{ GeV}/c$. The muon trigger extends over $|\eta| < 2.1$.

Significant contributions to both detectors are planned to be made by U.S. groups. For ATLAS, these groups involve about 200 physicists and engineers from 27 U.S. institutions; for CMS, about 300 physicists and engineers from 37 U.S. institutions. Contributions to ATLAS include one half to one third of the silicon pixels, one third to one quarter of the silicon strips, and the barrel transition radiation tracker; all or part of the readout for the liquid argon calorimeter, the EM section of the forward calorimeters, and about one third of the scintillator tile calorimeter; the endcap muon system, and contributions to the level 1 and level 2 triggers. For CMS, the list includes the forward silicon pixels, the hadron calorimeter system (management of the whole project and construction of the barrel and forward calorimeters); the EM calorimeter front-end; the endcap muon detectors (management of the system) and contributions to the level 1 and level 2 triggers (including management of the calorimeter trigger). At the time of writing (June 1996) negotiations are still ongoing between CERN and the U.S. funding agencies over the level of financial contribution to be made to ATLAS and CMS. Until final figures are arrived at, the contributions of U.S. groups are of course subject to revision.

One important, but less tangible, contribution from the U.S. groups is their involvement in the Tevatron collider program

with the CDF and DØ experiments. These provide a unique opportunity to learn, in a somewhat less demanding environment, how to deal with many of the challenges of high luminosity hadron collider physics, such as energy from pileup events, discrimination between multiple vertices, trigger rates dominated by backgrounds, and heavy flavor tagging, in a real experiment.

III. Higgs Physics

We will use “Higgs bosons” to refer to any scalar particles whose existence is connected to electroweak symmetry breaking. Generically, Higgs bosons couple most strongly to heavy particles. Their production cross section in hadron colliders is small resulting in final states with low signal to background ratios. The ability to detect them and measure their mass provides a set of benchmarks by which detectors can be judged. A specific model is required in order to address the quantitative questions of how well the detector can perform. While one may not believe in the details of any particular model, a survey of them will enable general statements to be made about the potential of the LHC and its detectors.

A. Standard Model Higgs

All the properties of the standard model Higgs boson are determined once its mass is fixed. The search strategy at LHC is therefore well defined. The current limit on the mass of the Higgs boson is $M_H > 65 \text{ GeV}$ for experiments at LEP[23]. Before the LHC gives data, masses up to 95 GeV will have been excluded or discovered by LEP[24]. There are several relevant production mechanisms; $gg \rightarrow H$ via an intermediate quark or gauge boson loop; $q\bar{q} \rightarrow WH$; $gg \rightarrow t\bar{t}H$; $gg \rightarrow b\bar{b}H$ and $qq \rightarrow qqH$. The relative importance of these processes depends upon the Higgs mass, the first dominates at small mass and the last at high masses. The branching ratios are shown in Fig. 3.

1. $H \rightarrow \gamma\gamma$ and associated production channels

At masses just above the range probed by LEP, the dominant decay of the Higgs boson is to the $b\bar{b}$ final state which is difficult to reconstruct. The decay to $\gamma\gamma$ is the most promising in this region. The branching ratio is very small and there is a large background from the pair production of photons via $q\bar{q} \rightarrow \gamma\gamma$, $gg \rightarrow \gamma\gamma$, and the bremsstrahlung process $qg \rightarrow q(\rightarrow \gamma)\gamma$. Excellent photon energy resolution is required to observe this signal, and this process is one that drives the very high quality electromagnetic calorimetry of both experiments.

CMS has a mass resolution of order 540 (870) MeV at $m_H = 110$ for low (high) luminosity[25]. The mass resolution is worse at high luminosity due to event pile up and the presence of a preshower detector that is used to determine the photon direction. This preshower is necessary as there are multiple interactions and the primary vertex is not readily recognised. The preshower enables the photon direction to be determined with a precision of $40 \text{ mrad}/\sqrt{E}$ and used to resolve the ambiguity in which of the several events contains the signal and therefore what point along the beam is used in computing the diphoton invariant mass. It is not present at low luminosity. The ATLAS

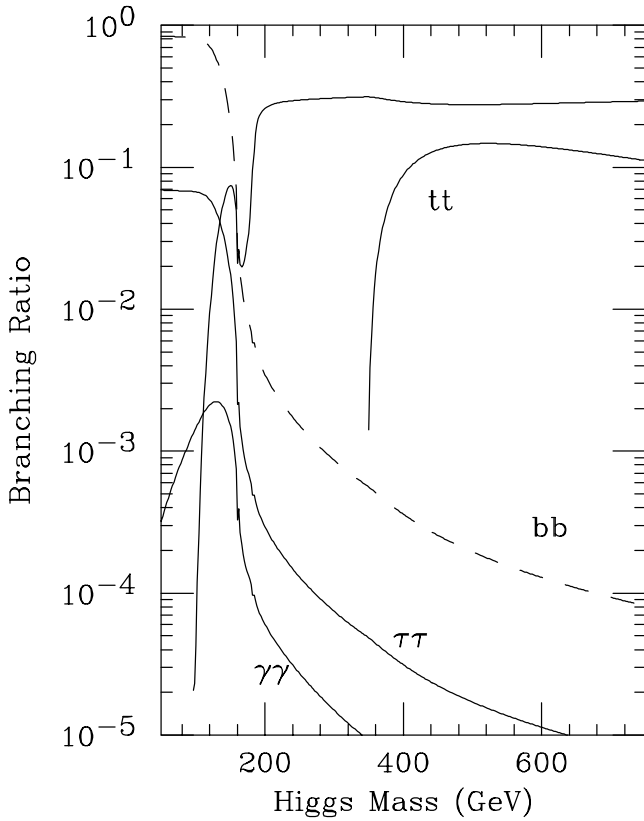


Figure 3: The branching ratios of the standard model Higgs boson as a function of its mass. The highest lying curve at large mass is the ZZ final state. Not shown is the WW rate which makes up almost all of the unaccounted for branching ratios.

mass resolution at high (low) luminosity is 1.2 (1.1) GeV for at $M_H = 110$ GeV. However the photon acceptance and identification efficiency are higher in the ATLAS analysis[26], partly because CMS rejects photons that convert in the inner detector.

In addition to the background from $\gamma\gamma$ final states, there are $jet - \gamma$ and $jet - jet$ final states, that are much larger. A jet/γ rejection factor of $\sim 10^3$ is needed to bring these backgrounds below the irreducible $\gamma\gamma$ background. A detailed GEANT based study of the ATLAS detector has been performed to study these backgrounds[26]. Jets were rejected by applying cuts on the hadronic leakage, photon isolation and the measured width of the electromagnetic shower. These cuts result in an estimate of these backgrounds which is a factor of six below the irreducible $\gamma\gamma$ background. The background $Z \rightarrow e^+e^-$ where both electrons are misidentified as photons was found to be significantly below the jet background, except in the range $m_H \sim m_Z$. In this case, stringent track rejection is needed. Given the uncertainties in the rates for these “reducible” backgrounds one can be confident that they are smaller than the irreducible $\gamma\gamma$ background, but they may not be negligible.

The CMS analysis for this process is as follows[2, 25]. Two isolated photons are required one of which has $p_T > 25$ GeV and the other has $p_T > 40$ GeV. Both are required to satisfy $|\eta| < 2.5$. Isolation means that there is no track or additional electromagnetic energy cluster with $p_T > 2.5$ GeV in a cone

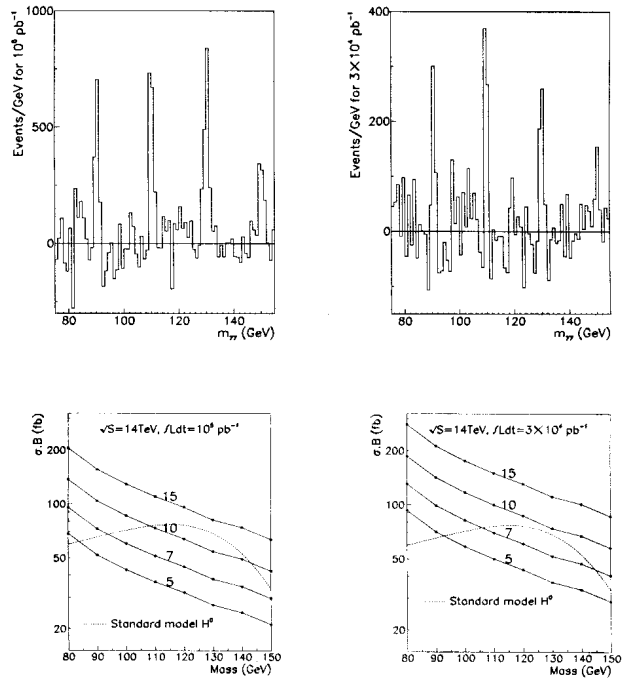


Figure 4: (a) The invariant mass distribution of $\gamma\gamma$ pairs as simulated by the CMS collaboration. A smooth background has been fitted and subtracted. (b) Curves showing the statistical significance of the peak as a function of the Higgs mass and the product of production cross-section and branching ratio σB . The dotted line corresponds to the value of σB as a function of the standard model Higgs boson mass. The left (right) figures correspond to low (high) luminosity running.

of size $\Delta R = 0.3$ around the photon direction. The Higgs signal then appears as a peak over the smooth background. The signal to background ratio is small, but there are many events. A curve can be fitted to the smooth background and subtracted from data. Fig. 4 shows the result of this subtraction. Peaks are shown corresponding to Higgs masses of 90, 110 and 130 GeV. The figure also shows the event rate needed to establish a signal of some significance as a function of the mass. From this one can see that this mode can discover the Higgs if its mass is too high to be detected at LEP and below about 140 GeV. At larger masses the branching ratio becomes too small for a signal to be extracted. The large event rate for this process implies that it becomes effective for a more limited range of Higgs masses once the integrated luminosity exceeds ~ 10 fb $^{-1}$. Results of the ATLAS study are similar and the reach of the two experiments is similar[26]

Another process is available at the lower end of the mass range. If the Higgs is produced in association with a W or $t\bar{t}$, the cross section is substantially reduced, but the presence of additional particles proportionally larger reduction in the background. Events are required to have an isolated lepton arising from the decay of the W (or top quark). This lepton can be used to determine the vertex position. The process is only useful at

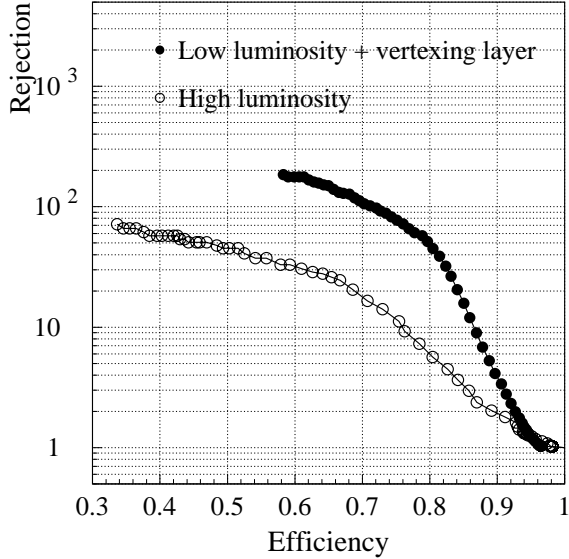


Figure 5: Rejection factor for light quark jets as a function of the tagging efficiency for b-quark jets in the ATLAS detector[1].

high luminosity, for 10^5 pb^{-1} there are approximately 15 signal events for Higgs masses between 90 and 120 GeV (the falling cross-section is compensated by the increased branching ratio for $H \rightarrow \gamma\gamma$) over an approximately equal background [27, 1]. The process will therefore provide confirmation of a discovery made in the $\gamma\gamma$ final state without an associated lepton.

1. $H \rightarrow b\bar{b}$

The dominant decay of a Higgs boson if its mass is below $2M_W$ is to $b\bar{b}$. The signal for a Higgs boson produced in isolation is impossible to extract. There is, as yet, no conceivable trigger for the process and the background production of $b\bar{b}$ pairs is enormous. The production of a Higgs boson in association with a W or $t\bar{t}$ pair can provide a high p_T lepton that can be used as a trigger. A study was conducted by ATLAS of this very challenging channel[28]. Events were triggered by requiring a muon (electron) with $|\eta| < 2.5$ and $p_T > 6(20)$ GeV. A study was carried out of the tagging efficiency to be expected for jets containing b-quarks[29]. $t\bar{t}$ events were generated and used both as a source of b-jets and light quark jets. At low luminosity, the ATLAS detector has a layer (the so-called B-layer) at ~ 5 cm from the beam. In this case a b-tagging efficiency of 70% is achieved with a rejection factor of 100 against light quark jets. The situation is somewhat worse at high luminosity as is shown in Fig. 5 This b-tagging efficiency is not significantly larger than that obtained by CDF[30].

The study of $H \rightarrow b\bar{b}$ assumed an efficiency of 50% and a background rejection of 100. Using this assumption the background from $Wb\bar{b}$ events is slightly larger than that from W's

in association with light quark jets. The Higgs search is then limited by the background from real b-quarks which is detector independent. Jets were retained if they had $p_T > 16$ GeV and $|\eta| < 2.5$. In order to reduce the background from $t\bar{t}$ events a veto was applied to reject events with a second isolated lepton $p_T > 6$ GeV and $|\eta| < 2.5$ and additional jets with $p_T > 15$ GeV in $|\eta| < 5$. For a luminosity of 10^4 pb^{-1} , there are 175, 110 and 47 signal events for Higgs masses of 80, 100 and 120 GeV from the WH process. The reconstructed $b\bar{b}$ mass distribution is not gaussian, it has a tail on the low side. Nevertheless fit to a gaussian gives $\sigma \sim 11$ GeV for a mass of 100 GeV. The position of the peak is also shifted down by about 20%. These two degradations are caused mainly by gluon radiation off the final state b quarks and losses due to decays. The background arising from $Wb\bar{b}$ events is large; approximately 3000, 2500 and 1880 events in a bin of width 40 GeV centered on the reconstructed $b\bar{b}$ mass peak. An additional background from $WZ(\rightarrow b\bar{b})$ is present if $m_H \sim M_Z$ and contributes an event rate approximately equal to that of the signal. The final state $t\bar{t}H(\rightarrow b\bar{b})$ was also studied. A third tagged b-jet was required. The signal and background rates were similar to the WH case[28]. From this study we can draw the following conclusion. Extraction of a signal will be possible if at all only over a very limited mass range ($\sim 80 - 110$ GeV) and depends critically upon the b-tagging efficiency and background rejection. The signal may be sufficient to confirm the discovery of a Higgs in another channel.

1. $H \rightarrow ZZ^* \rightarrow 4\ell$

The search for the Standard Model Higgs relies on the four-lepton channel over a broad mass range from $m_H \sim 130$ GeV to $m_H \sim 800$ GeV. Below $2m_Z$, the event rate is small and the background reduction more difficult, as one or both of the Z-bosons are off-shell. In this mass region the Higgs width is small ($\lesssim 1$ GeV) and so lepton energy or momentum resolution is of great importance in determining the significance of a signal[32].

For $m_H < 2m_Z$, the main backgrounds arise from $t\bar{t}$, $Zb\bar{b}$ and continuum $Z(Z/\gamma)^*$ production. Of these, the $t\bar{t}$ background can be reduced by lepton isolation and by lepton pair invariant mass cuts. The $Zb\bar{b}$ background cannot be reduced by a lepton pair invariant mass cut but can be suppressed by isolation requirements. The ZZ^* process is an irreducible background. Both CMS and ATLAS studied the process for $m_H = 130, 150$ and 170 GeV. Signal events were obtained from both $gg \rightarrow H$ and WW/ZZ fusion processes, giving consistent cross sections $\sigma \cdot B \approx 3, 5.5$ and 1.4 fb respectively (no K-factors being included).

In the CMS study[2, 31] event pileup appropriate to $\mathcal{L} = 10^{34} \text{ cm}^{-2}\text{s}^{-1}$ was modelled by superimposing 15 minimum bias events (simulated by QCD dijets with $p_T \geq 5$ GeV/c). The muon resolution was obtained from a full simulation of the detector response and track-fitting procedure. This was then parameterized as a function of p_T and η . Internal bremsstrahlung was generated using the PHOTOS program and leads to about 8% of reconstructed $Z \rightarrow \mu^+\mu^-$ pairs falling outside a $m_Z \pm 2\sigma_Z$ window for $m_H = 150$ GeV. The reconstructed $\mu^+\mu^-$

mass has a resolution $\sigma_Z = 1.8$ GeV in the Gaussian part of the peak. The electron resolution was obtained from a detailed GEANT simulation of the calorimeter, including the effects of material in the beampipe and the tracker, and the reconstruction of electron energy in the crystal calorimeter. Including internal and external bremsstrahlung, and using a 5×7 crystal matrix to reconstruct the electron, the mass resolution $\sigma_Z = 2.3$ GeV and the reconstruction efficiency is about 70% (within $m_Z \pm 2\sigma_Z$).

Events were selected which had one electron with $p_T > 20$ GeV/c, one with $p_T > 15$ GeV/c and the remaining two with $p_T > 10$ GeV/c, all within $|\eta| < 2.5$. For muons, the momenta were required to exceed 20, 10 and 5 GeV/c within $|\eta| < 2.4$. One of the e^+e^- or $\mu^+\mu^-$ pairs was required to be within $\pm 2\sigma_Z$ of the Z mass. This cut loses that fraction of the signal where both Z 's are off-shell, about a 24% inefficiency at $m_H = 130$ GeV and 12% at $m_H = 170$ GeV. The two softer leptons were also required to satisfy $m_{\ell\ell} > 12$ GeV. Additional rejection is obtained by requiring that any three of the four leptons be isolated in the tracker, demanding that there is no track with $p_T > 2.5$ GeV/c within the cone $R < 0.2$ around the lepton. This requirement is not very sensitive to pileup as the 2.5 GeV/c threshold is quite high. This yields signals at the level of 7.4, 15.2 and 5.0 standard deviations for $m_H = 130, 150,$ and 170 GeV in $2 \times 10^5 \text{ pb}^{-1}$.

The ATLAS[1, 32] study followed a similar technique. The detector resolutions and reconstruction efficiencies were obtained using detailed detector simulations, including the effects of pileup. For the four-electron mode, the Higgs mass resolution at $m_H = 130$ GeV is 1.7 (1.5) GeV at high (low) luminosity, including the effect of electronic noise in the calorimeter. For muons, the corresponding figure is 2.0 GeV after correcting for muon energy losses in the calorimeter; this can be improved to about 1.6 GeV by combining the muon momentum measured in the muon system with that obtained from the central tracker after the tracks have been matched. Events were selected which had two leptons with $p_T > 20$ GeV/c, and the remaining two with $p_T > 7$ GeV/c, all within $|\eta| < 2.5$. One of the e^+e^- or $\mu^+\mu^-$ pairs was required to be within ± 6 GeV of the Z mass. The two softer leptons were also required to satisfy $m_{\ell\ell} > 20$ GeV.

ATLAS used a combination of calorimeter isolation and impact parameter cuts. The isolation criterion is that the transverse energy within $R = 0.3$ of the lepton be less than E_T^{cut} . Values of E_T^{cut} of 3, 5, and 7 GeV were used for $4\mu, ee\mu\mu$ and $4e$ modes at 10^{33} (10^{34}) luminosity to obtain a constant signal efficiency of 85% (50%). Tighter cuts can be used for muons because they do not suffer from transverse leakage of the EM shower. The impact parameter, as measured in the silicon tracker, is used to further reduce the background from heavy flavor processes ($t\bar{t}$ and $Zb\bar{b}$)[32]. ATLAS obtain signals at the level of 8.5 (7.8), 22 (18) and 6.5 (5) standard deviations for $m_H = 130, 150,$ and 170 GeV in 10^5 pb^{-1} ($3 \times 10^4 \text{ pb}^{-1}$). The four-lepton mass distributions are shown in Fig. 6.

1. $H \rightarrow ZZ \rightarrow 4\ell$

The $H \rightarrow ZZ \rightarrow 4\ell$ channel is sensitive over a wide range of Higgs masses from $2m_Z$ upwards: to about 400 GeV with

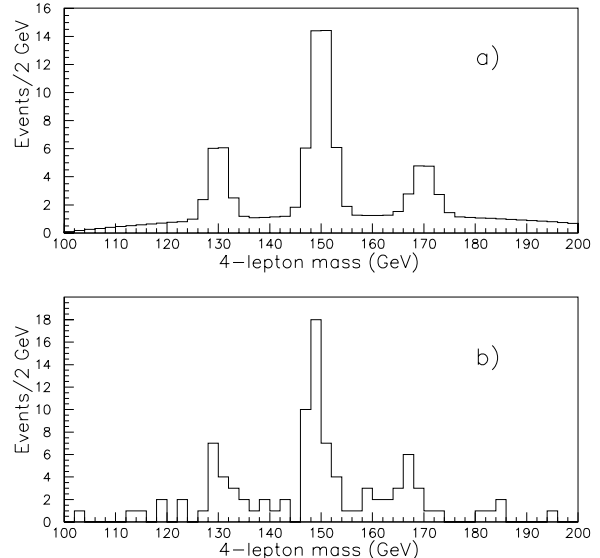


Figure 6: Reconstructed four-lepton mass above background, for $m_H = 130, 150$ and 170 GeV, and an integrated luminosity of $3 \times 10^4 \text{ pb}^{-1}$ (low luminosity) as simulated by the ATLAS collaboration. (a) indicates the expected average number of events; (b) shows the result of one experiment, obtained with randomized statistics in each mass bin.

10^4 pb^{-1} and to about 600 GeV with 10^5 pb^{-1} . For lower Higgs masses, the width is quite small and precision lepton energy and momentum measurements are helpful; for larger masses the natural Higgs width becomes large. The main background is continuum ZZ production.

CMS[2, 31] studied the process for $m_H = 300, 500$ and 600 GeV. The electron and muon resolutions and the selection cuts were the same as used for the ZZ^* channel. Internal and external bremsstrahlung were simulated using the PHOTOS program and a GEANT detector simulation. Two e^+e^- or $\mu^+\mu^-$ pairs with a mass within ± 6 GeV of m_Z were required. No isolation cut was imposed as the remaining backgrounds are small. The resulting 4-lepton invariant mass distributions are shown in Fig. 7. With 10^5 pb^{-1} a signal in excess of six standard deviations is visible over the entire range $200 < m_H < 600$ GeV. ATLAS obtains very similar results[1].

1. $H \sim 1 \text{ TeV} (\ell\nu\nu, \ell\ell jj, \ell\nu jj, \text{etc.})$

As the Higgs mass is increased further, its width increases and the production rate falls and one must turn to decay channels that have a larger branching ratio. The first of these is $H \rightarrow ZZ \rightarrow \ell\nu\bar{\nu}$. Here the signal involves looking for a Z decaying to lepton pairs and a large amount of missing energy. The signal appears as a Jacobian peak in the missing E_T spectrum. There are more potentially important sources of background in this channel than in the 4ℓ final state. In addition to the irreducible background from ZZ final states, one has to worry about $Z + jets$ events where the missing E_T arises from

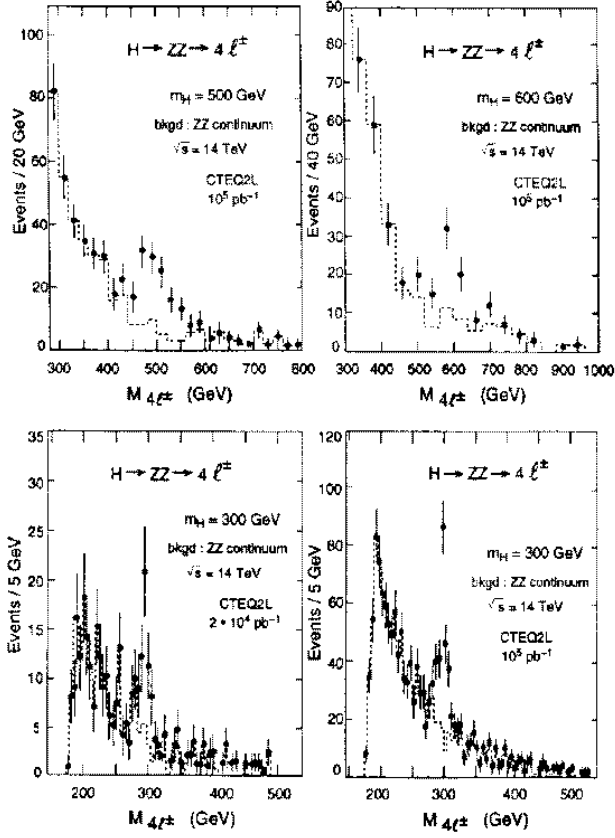


Figure 7: Mass distribution in $H \rightarrow ZZ^* \rightarrow 4\mu$ for $M_H = 150$ GeV as simulated by CMS including all bremsstrahlung losses.

neutrinos in the jets or from cracks and other detector effects that cause jet energies to be mismeasured. At high luminosity the background from the pile up of minimum bias events produces a E_T^{miss} spectrum that falls very rapidly and is completely negligible for $E_T^{miss} > 100$ GeV, provided the calorimeter extends to $|\eta| < 5$. ATLAS conducted [34] a full GEANT based study of this background for which 5000 high transverse momentum $Z + jet$ events were fully simulated. The events were selected so that a large fraction of them had jets going into the region $0.9 < |\eta| < 1.3$ where ATLAS has weaker jet energy resolution due to the crack between the endcap and barrel hadron calorimeters. The dominant part of the $Z + jets$ background that remains is that where the missing E_T arises from the semi-leptonic decays of b-quarks in the jets. The contribution from detector effects is not dominant.

Figure 8 shows the missing E_T spectrum at high luminosity (10^5 pb^{-1}). On this plot the $Z + jets$ background is estimated from a parton level simulation as there are insufficient statistics in the full study to obtain the full missing E_T spectrum. This estimate correctly models the contribution from b-decays which the full study showed to be dominant. A cut was imposed requiring that reconstructed $Z \rightarrow \ell\ell$ has $p_T(Z) > 250$ GeV. This cut causes the ZZ background to peak. This effect is less pronounced if a cut is made on E_T^{miss} and then the plot is remade

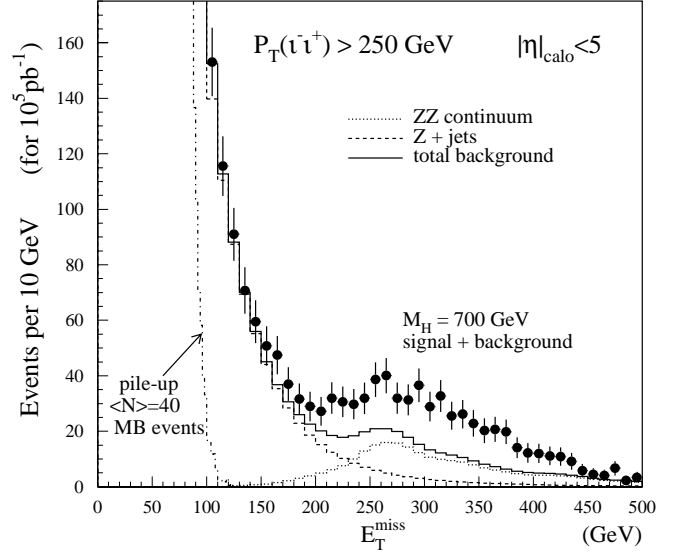


Figure 8: Missing E_T spectrum for the $H \rightarrow ZZ \rightarrow \ell\ell\nu\bar{\nu}$ process. The background contributions are shown separately; $Z + jets$ (dashed); ZZ (dotted) and minimum bias pile up (dot-dashed). The signal due to a Higgs boson of mass 700 GeV.

with $p_T(Z)$ on the abscissa. The statistical significance of the signal shown is large but it is difficult to assess at this stage the true significance when data are actually taken. The dominant ZZ background has QCD corrections of order 40% [37]. Once data are available this background will be measured. The CMS analysis of this process[2, 35] uses a central jet veto requiring that there be no jets with $E_T > 150$ GeV within $|\eta| < 2.4$. By requiring a jet in the far forward region (see below), most of the remaining ZZ background can be rejected. A study by CMS requiring a jet with $E > 1\text{TeV}$ and $2.4 < |\eta| < 4.7$, produces an improvement of approximately a factor of three in the signal to background ratio at the cost of some signal. This mode is only effective for high mass higgs bosons and becomes powerful only at high luminosity. Nevertheless it will provide an unambiguous signal.

Substantially larger event samples are available if the decay modes $H \rightarrow WW \rightarrow \ell\nu + jets$ and $H \rightarrow ZZ \rightarrow \ell\ell + jets$ can be exploited efficiently. In order to do this one has to reduce the enormous $W + jets$ and $Z + jets$ background by kinematic cuts. Henceforth the discussion will be for the WW final state; the ZZ state is similar. The first step is to reconstruct the W decay to jets[38]. A particle level simulation was used including the effects of pile up at high luminosity. Basic calorimeter cells of $\Delta\phi \times \Delta\eta = 0.05 \times 0.05$ and energy threshold of $E_T = 1$ GeV per cell were used. Jets were found using a cone of size $\Delta R = 0.5$ and required to have $E_T > 350$ GeV. Within these cones two smaller jets with $\Delta R = 0.2$ and $E_T > 50$ GeV were reconstructed. This algorithm reconstructs $W \rightarrow jets$ with an efficiency of about 60% and a W mass resolution of approximately 6.5 GeV for W 's produced in the decay of 1

Process	Central cuts	Jet veto	Single tag	Double tag
$H \rightarrow WW$	364	251	179	57
$t\bar{t}$	5620	560	110	5
$W + jets$	9540	3820	580	12
pileup			160	2

Table I: $H \rightarrow WW \rightarrow \ell\nu jj$ signals and backgrounds, for $m_H = 1$ TeV, before and after cuts in the forward region (see text). The rates are computed for an integrated luminosity of 10^5 pb^{-1} and a lepton efficiency of 90%. Only the $qq \rightarrow Hqq$ contribution to the signal is included. Table from an ATLAS simulation.

TeV Higgs bosons. The mass resolution is slightly better at low luminosity where pile up is unimportant. These cuts applied to the $W(\rightarrow \ell\nu) + jets$ sample with $p_T(W) > 200$ GeV reduces the rate for this process by a factor of 500 and brings it to a level approximately equal to that from $t\bar{t} \rightarrow WbW\bar{b}$. A limited statics full simulation of this method in the ATLAS detector is in qualitative agreement with the above study [1].

After these cuts, the backgrounds from $W + jets$ and $t\bar{t}$ are still larger than the signal from $H \rightarrow WW$ and topological cuts are required. One of the processes $qq \rightarrow Hqq$ produces the Higgs boson in association with jets at large rapidity. These jets can be used as a tag to reject background. This forward jet tag will cause some loss of signal since the $gg \rightarrow H$ process lacks these forward jets. Hence it is only effective for high mass Higgs bosons where the $qq \rightarrow Hqq$ process is a significant part of the cross section. The central part (in rapidity) of the Higgs events is expected to have less jet activity in it than the background, particularly that background from $t\bar{t}$. At low luminosity, requiring that the events have no additional jets (apart from the ones that make up the W candidate) with $E_T > 15$ GeV and $|\eta| < 2$ loses approximately 30% of the signal and reduces the background from $W + jets$ ($t\bar{t}$) by a factor of 3 (30). At high luminosity the requirement has to be raised to $E_T > 40$ GeV in order to preserve the efficiency for the signal. The rejection factors for $W + jets$ and $t\bar{t}$ are then 2.5 and 12.

The forward jet tagging was investigated in ATLAS as follows. Clusters energy of size $\Delta R = 0.5$ were found in the region $2 < |\eta| < 5$. Events from the pile up of minimum bias events have jets in this regions so the threshold on E_T of the jet must be set high enough so that these jets do not generate tags in the background. If the individual calorimeter cells are required to have $E_T > 3$ GeV, then there is there is a 4.6% (0.07%) probability that the pile up at high luminosity will contribute a single (double) tag to an event that would otherwise not have one for tagging jets with $E_T > 15$ GeV and $E > 600$ GeV. The requirements for single and double tags are then applied to the signal from a Higgs boson of mass 1 TeV and the various backgrounds. The pile up contributions are included and the event rates for a luminosity of 10^5 pb^{-1} shown in table I.

It can be seen from the table that it may be possible to extract a signal but the quoted signal to background ratios should

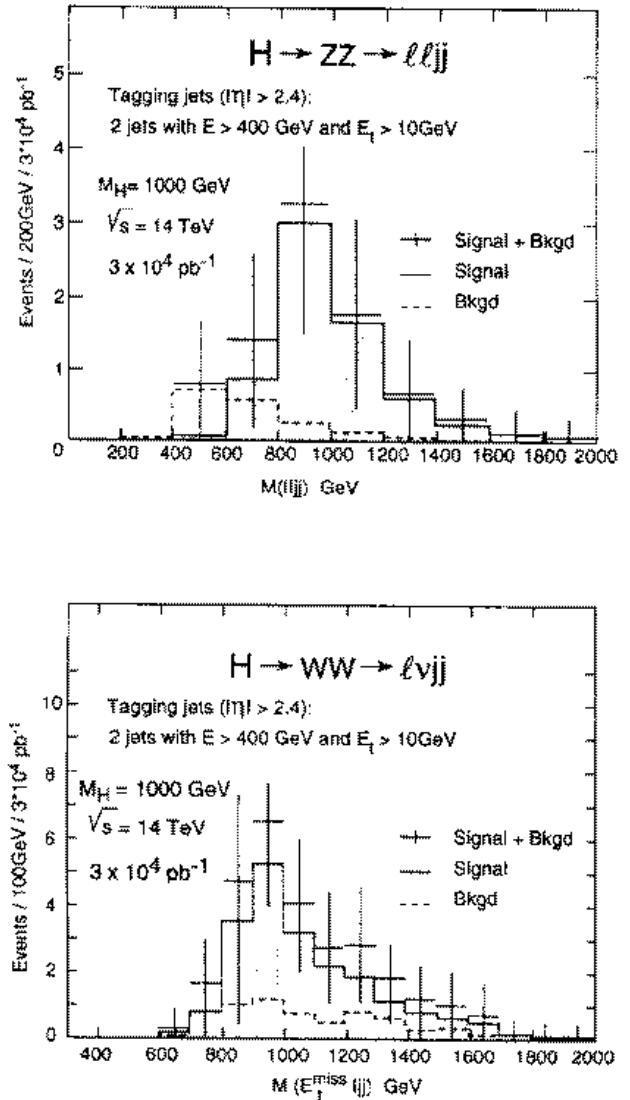


Figure 9: Reconstructed diboson mass distributions in the final states $\ell\ell jj$ and $\ell\nu jj$ showing a peak from a 1 TeV Higgs boson from a CMS simulation.

not be taken too seriously. However, other kinematic quantities may be used to further discriminate between the signal and the background. The ZZ final state is cleaner as there is no $t\bar{t}$ background but the event rates are much smaller.

A separate study was performed by the CMS group[2, 36]. Here two tagging jets with $|\eta| > 2.4$, $E_T > 10$ GeV and $E > 400$ GeV are required. Two central jets are required with in invariant mass within 15 GeV of the W or Z mass. For the ZZ case, the Z is reconstructed from e or μ pairs with invariant mass within 10 GeV of the Z mass; each lepton has $p_T > 50$ GeV and the pair has $p_T > 150$ GeV. For the WW case, at least 150 GeV of missing E_T is needed and the charged lepton from the W has $p_T > 150$ GeV. The result of this study is shown in Fig. 9.

1. Summary of standard model Higgs

The LHC at full luminosity will be able to probe the entire range of allowed Higgs masses from the value reachable by LEP up to the value where it is no longer sensible to speak of an elementary Higgs boson using final states that one is absolutely confident will be effective: $\gamma\gamma$, $A\ell$ and $2\ell\nu\bar{\nu}$. Additional final states that afford an excellent chance of having a signal will be exploited to support these; $b\bar{b}$ and $\ell\nu + jets$, $\ell\ell + jets$. The failure to find a boson over this range would therefore enable the standard model to be ruled out. The Higgs sector then either consists of non-standard Higgs bosons or the electroweak symmetry breaking is via some strongly coupled process that will manifest itself in the study of WW scattering. The next subsection is devoted to an example of the former type.

B. SUSY Higgs

As stated above the minimal supersymmetry model (MSSM) has three neutral and one charged Higgs bosons; h , H , A and H^\pm . These arise because supersymmetric models, unlike the standard model, need different Higgs bosons to generate masses for the up and down type quarks. In the standard model one parameter, the Higgs mass, is sufficient to fully fix its properties. In the Minimal supersymmetric model, two parameters are needed. These can be taken to be the mass of A which is unconstrained, and the ratio ($\tan\beta$) of the vacuum expectation values of the Higgs fields that couple to up-type and down-type quarks. If $\tan\beta$ is $O(1)$, then coupling of the top quark to Higgs bosons (λ_t) is much larger than that of bottom quarks (λ_b) as is the case in the standard model.

None of these Higgs bosons has been observed, so we need consider only the regions of parameter space not yet excluded. The masses of h and H are given in terms of the mass of A and $\tan\beta$. The charged Higgs boson H^\pm is heavier than A ($M_{H^\pm}^2 \sim M_A^2 + M_W^2$). H is heavier than A and, at large values of M_A A and H , become almost degenerate. The mass of the lightest boson, h , increases with the mass of A and reaches a plateau for A heavier than about 200GeV. The actual values depend on the masses of the other particles in the theory particularly the top quark [39]. There is also a dependence (via radiative corrections) on the unknown masses of the other supersymmetric particles. This dependence is small if these particles are heavy, so it is conventional to assume that this is the case. The only uncertainty in the masses of the Higgs bosons then arises from the error on the top quark mass. Unfortunately the upper bound on the mass of h is such that it might be out of the range of LEP, which is 95 GeV for small $\tan\beta$ and 88 GeV for large $\tan\beta$.

In the limit of large A mass, the couplings of the Higgs bosons are easy to describe. The couplings of h become like those of the standard model Higgs boson. This raises the possibility that if h is observed at LEP, it may not be possible to distinguish it from those of the standard model Higgs boson. The couplings of A and H to charge 1/3 quarks and leptons are enhanced at large $\tan\beta$ relative to those of a standard model Higgs boson of the same mass. However, A does not couple to gauge boson pairs and the coupling of H to them is suppressed at large $\tan\beta$

and large M_A . The decay modes used above in the case of the standard model Higgs boson can also be exploited in the SUSY Higgs case. h can be searched for in the final state $\gamma\gamma$, as the branching ratio approaches that for the standard model Higgs in the large M_A (decoupling) limit.

The decay $A \rightarrow \gamma\gamma$ can also be exploited. This has the advantage that, because $A \rightarrow ZZ$ and $A \rightarrow WW$ do not occur, the branching ratio is large enough for the signal to be useable for values of M_A less than $2m_t$ [40]. The decay $H \rightarrow ZZ^*$ can be exploited, but at large values of M_H the decay $H \rightarrow ZZ$, which provides a very clear signal for the standard model Higgs, is useless owing to its very small branching ratio. The decays of $h \rightarrow b\bar{b}$ can also be exploited.

In addition to these decay channels, several other possibilities open up due to the larger number of Higgs bosons and possibly enhanced branching ratios. The most important of these are the decays of H and A to $\tau^+\tau^-$ and $\mu^+\mu^-$, $H \rightarrow hh$, $A \rightarrow Zh$ and $A \rightarrow t\bar{t}$.

2. $H/A \rightarrow \tau\tau$

In the MSSM, the $H \rightarrow \tau^+\tau^-$ and $A \rightarrow \tau^+\tau^-$ rates are strongly enhanced over the standard model if $\tan\beta$ is large, resulting in the possibility of observation over a large region of parameter space. The $\tau^+\tau^-$ signature can be searched for either in a lepton+hadron final state, or an $e + \mu$ final state. As there are always neutrinos to contend with, mass reconstruction is difficult, and E_T^{miss} resolution is critical. In ATLAS, at high luminosity this resolution is $\sigma(E_{T,x}^{miss}) = \sigma(E_{T,y}^{miss}) = 1.1/\sqrt{\sum E_T}$. Irreducible backgrounds arise from Drell-Yan tau pair production, $t\bar{t} \rightarrow \tau\tau$ and $b\bar{b} \rightarrow \tau\tau$. Both CMS[41] and ATLAS[42] have studied $\tau^+\tau^-$ final states using full simulation.

For the lepton+hadron final state, there are additional reducible backgrounds from events with one hard lepton plus a jet which is misidentified as a tau. In the CMS and ATLAS studies, events were required to have one isolated lepton with $p_T > 15 - 40$ GeV depending on m_A (CMS) or $p_T > 24$ GeV (ATLAS) within $|\eta| < 2.0(2.4)$ and one tau-jet candidate within $|\eta| < 2.0(2.5)$. A lepton reconstruction efficiency of 90% was assumed by both ATLAS and CMS.

CMS identified tau-jets by requiring $50 < E_T < 120$ GeV for $m_A < 300$ GeV and $E_T > 60$ GeV for $m_A > 300$ GeV. Exactly one charged track with $p_T > 25 - 40$ GeV/c was required within $R = 0.1$ of the jet axis, and no tracks with $p_T > 2.5$ GeV/c in the annulus between $R = 0.1$ and $R = 0.4$. ATLAS required that the tau jet have $E_T > 40$ GeV, that the radius of the jet computed from the EM cells only be less than 0.07; that less than 10% of its transverse energy be between $R = 0.1$ and $R = 0.2$ of its axis; and again, that exactly one charged track with $p_T > 2$ GeV/c point to the cluster. The CMS and ATLAS selections are about 40%(26%) efficient for taus, while accepting only 1/100 (1/400) of ordinary light quark and gluon jets.

CMS vetoed events having other jets with $E_T > 25$ GeV within $|\eta| < 2.4$ (this reduces the $t\bar{t}$ background); while ATLAS used cuts on E_T^{miss} , the transverse mass of the lepton and

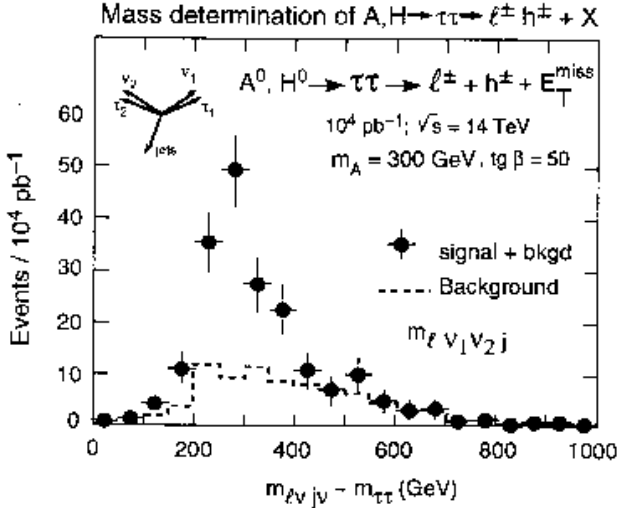


Figure 10: Invariant mass distribution of the $\ell j \nu \nu$ system for selected events with $m_A = 300$ GeV and $\tan \beta = 50$ from CMS.

E_T^{miss} , and the azimuthal angle between the lepton and the tau-jet. The mass of the higgs may be reconstructed by assuming the neutrino directions to be parallel to those of the lepton and the tau-jet. Resolutions of 12 and 14 GeV (Gaussian part) are obtained by ATLAS and CMS for $m_A = 100$ GeV. The reconstructed higgs peak is shown in Fig.10.

For the $e + \mu$ final state, CMS required a pair of opposite-sign unlike-flavor leptons with $p_T > 20$ GeV/c and $|\eta| < 2.0$. There are large backgrounds from the tau-pair processes listed above plus WW production. The $t\bar{t}$ and WW processes can be reduced to about one-fifth the Drell-Yan tau-pair rate by a calorimeter circularity cut and by requiring $\Delta\phi$ between the leptons be greater than 130° . The signal efficiency is about 40%. Both ATLAS and CMS find the sensitivity in the $e + \mu$ final state to be less than for the lepton+hadron final state, owing to its smaller rate and less favorable decay kinematics.

Taking the lepton+hadron and $e + \mu$ modes together, for the sum of h , H and A decays, both ATLAS and CMS find that the large region of parameter space corresponding to $\tan \beta \gtrsim 6$ at $m_A = 125$ GeV rising to $\tan \beta \gtrsim 30$ at $m_A = 500$ GeV may be excluded at the 5σ confidence level with 3×10^4 pb $^{-1}$. ATLAS also finds some sensitivity to $\tan \beta \lesssim 2$ for $125 < m_A < 350$ GeV at very high integrated luminosities (3×10^5 pb $^{-1}$).

2. $H/A \rightarrow \mu\mu$

The branching ratio for H (or A) to $\mu^+\mu^-$ is smaller than that to $\tau^+\tau^-$ by a factor of $(m_\mu/m_\tau)^2$. The better resolution available in this channel compensates to some extent for this and the $\mu^+\mu^-$ mode can be useful for large values of $\tan \beta$. A signal of less statistical significance than that in the $\tau^+\tau^-$ could be used to confirm the discovery and make a more precise measurement of the mass and production cross section. The ATLAS analysis [43] requires two isolated muons with $p_T > 20$ GeV and

$|\eta| < 2.5$. The background from $t\bar{t}$ events is rejected by requiring $E_T^{miss} < 30(60)$ GeV at low (high) luminosity. A jet veto could be employed to reduce this background further, but this is ineffective at reducing the remaining dominant background for $\mu^+\mu^-$ pairs from the Drell-Yan process. A cut on the transverse momentum of the muon pair, requiring it to be more than 10 GeV for small Higgs masses and 20 GeV for larger masses reduces this background slightly. The remaining background is very large within ± 15 GeV of the Z mass. Above this region the signal appears as a narrow peak in the $\mu^+\mu^-$ mass spectrum. In this troublesome region the signal will be statistically significant if $\tan \beta$ is large enough but it appears as a shoulder on the edge of a steeply falling distribution which may make it more difficult to extract a signal.

The significance of the signal in this channel is determined by the $\mu^+\mu^-$ mass resolution and the intrinsic width of the Higgs resonance. The mass resolution in ATLAS is approximately $0.02m_A$ and $0.013m_A$ in CMS[44]. At large $\tan \beta$, the masses of A and H are almost degenerate and they cannot be resolved from each other. The natural width of A is proportional to $\tan^2 \beta$ and is approximately 3 GeV for $\tan \beta = 30$ and $M_A = 150$ GeV. The mode will provide a 4σ signal for a region in the $M_A - \tan \beta$ plane covering $M_A > 110$ GeV and $\tan \beta > 15$ for an integrated luminosity of 10^5 pb $^{-1}$.¹

2. $A \rightarrow \gamma\gamma$

The prospects for detecting the CP-odd Higgs boson (A) via its decay into photon pairs at the LHC were investigated at Snowmass[40]. The CMS detector performance was adopted for a realistic study of observability.

Gluon fusion ($gg \rightarrow A$) via top and bottom quark triangle loop diagrams is the dominant production process if $\tan \beta \lesssim 4$; while for large $\tan \beta$ ($\gtrsim 7$) b -quark fusion dominates. Both processes were included in this study. QCD corrections to the cross section were not included, but the effect of QCD radiative corrections on the branching fraction of $A \rightarrow b\bar{b}$ (which is reduced by about a factor of 2) was taken into account. For $\tan \beta \approx 1$ and $170 \text{ GeV} < m_A < 2m_t$ the branching fraction of $A \rightarrow \gamma\gamma$ is between 5×10^{-4} and 2×10^{-3} .

Events were simulated using PYTHIA 5.7 with the CTEQ2L parton distribution functions. The backgrounds considered are QCD photon production, both the irreducible two-photon backgrounds ($q\bar{q} \rightarrow \gamma\gamma$ and $gg \rightarrow \gamma\gamma$) and the reducible backgrounds with one real photon ($q\bar{q} \rightarrow q\gamma$, $qg \rightarrow q\gamma$, and $gg \rightarrow g\gamma$). Both photons were required to have transverse energy (E_T) larger than 40 GeV and $|\eta| < 2.5$. Both photons are required to be isolated, *i.e.*, (1) there is no charged particle in the cone in the cone $R = 0.3$; and (2) the total transverse energy $\sum E_T^{cell}$ is taken to be less than 5 GeV in the cone ring $0.1 < R < 0.3$. In this preliminary analysis, no rejection power was assumed against π^0 's with high E_T , and all π^0 's surviving the cuts are considered accepted. (This is very conservative and overestimates the background especially in the low mass $M_{\gamma\gamma}$ region.)

¹The CMS event rates appear larger than the ATLAS ones. CMS added the A and H rates whereas the ATLAS numbers correspond to the A alone.

Fig. 11 shows the reconstructed $\gamma\gamma$ mass above background for $m_A = 180, 200, 250, 300$ and 350 GeV and $\tan\beta = 1$. The higgs peaks are clearly visible. The 5σ discovery region for this channel in the $m_A - \tan\beta$ plane is also shown. Evidently this channel may provide a good opportunity to precisely reconstruct the CP-odd Higgs boson mass (m_A) for $170 \text{ GeV} < m_A < 2m_t$ if $\tan\beta$ is close to one. The impact of SUSY decays on this discovery channel might be significant and is under investigation with realistic simulations.

2. $H \rightarrow hh$

Observation of this channel would be particularly interesting as information about two different Higgs bosons and their coupling could be obtained. The dominant decay here is the to final state $b\bar{b}b\bar{b}$. However it is not clear how this mode could be triggered efficiently and there is a very large background from QCD events. The channel $H \rightarrow hh \rightarrow b\bar{b}\tau^+\tau^-$ would be triggerable if one tau decayed leptonically. This channel has not been studied.

The decay channel $H \rightarrow hh \rightarrow \gamma\gamma b\bar{b}$ is triggerable and was studied[43] recently. Events were required to have a pair of isolated photons with $|\eta| < 2.5$ and $p_T > 20$ GeV and two jets with $p_T > 15(30)$ GeV and $|\eta| < 2.5$ at low (high) luminosity. One of the jets was required to be tagged a b-jet and an efficiency of 60 (50) % assumed with a rejection of 100 (10) against light (charm) jets. The dominant background arises from $\gamma\gamma$ production in association with light quark jets and is approximately 10 times larger than the $\gamma\gamma b\bar{b}$ background. Event rates are very low, for $M_H \sim 230$ GeV and $m_h = 70$ GeV there are about 20 signal events at high luminosity. However the very small background (~ 2) and the sharp peak in the $\gamma\gamma$ mass distribution should provide convincing evidence of a signal.

2. Other possibilities

For large masses, the A and H decay almost exclusively to $t\bar{t}$. The background in this channel arises from $t\bar{t}$ production and is very large. A statistically significant signal can be extracted provided that the background can be calibrated [43]. For an integrated luminosity of 10^5 pb^{-1} there are about 9000 events for $M_A \sim 400$ GeV after, cuts requiring an isolated lepton (which provides the trigger) and a pair of tagged b-quark jets. The $t\bar{t}$ mass resolution is of order 70 GeV resulting in approximately 100000 background events. The rate for $t\bar{t}$ production is well predicted by perturbative QCD, so it may well be possible to convincingly establish an event excess but extraction of a mass for A will be very difficult. The mode is most likely to be useful as confirmation of a signal seen elsewhere.

The decay $A \rightarrow Zh$ affords another place where two Higgs bosons might be observed simultaneously. The leptonic decay of the Z can be used as a trigger. The CMS study requires a pair of electrons (muons) with $p_T > 20$ (5) which have an invariant mass within 6 GeV of the Z mass and a pair of jets with $p_T > 40$ GeV. One or two b-tags are required with an assumed efficiency of 40% and a rejection of 50 against light quark jets. The background is dominated by $t\bar{t}$ events.² The

²A K factor of 1.5 was included in the backgrounds shown on figure 12.

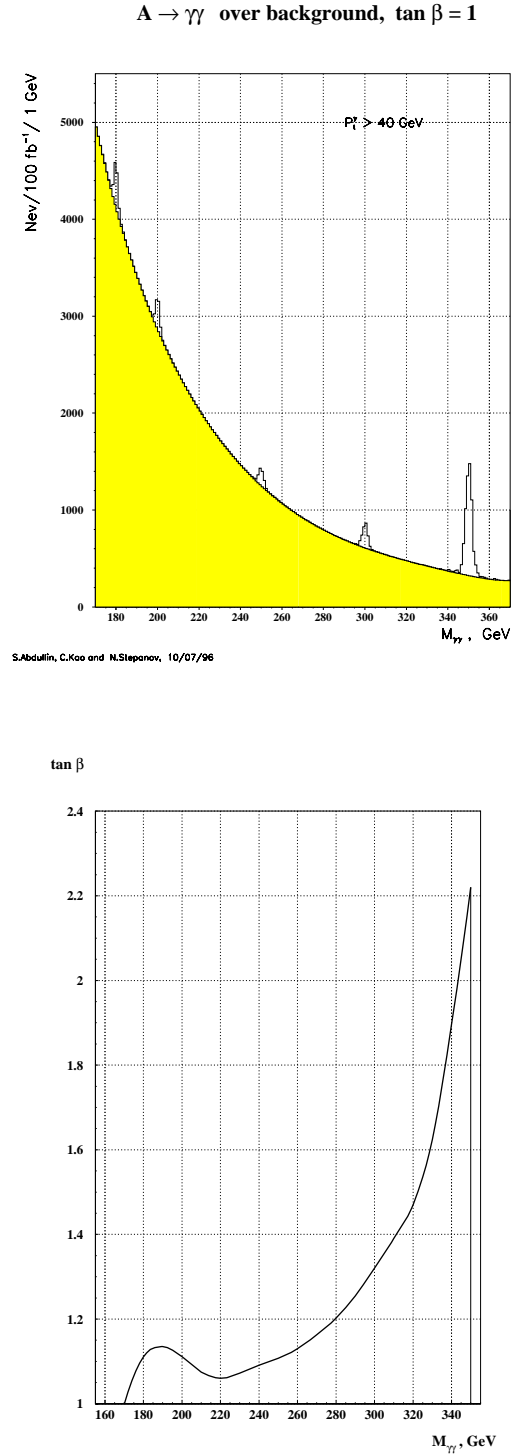


Figure 11: (a) Number of $A \rightarrow \gamma\gamma$ events above background for 100 fb^{-1} and $m_A = 180, 200, 250, 300$ and 350 GeV and $\tan\beta = 1$. (b) 5σ discovery region for this channel in the $m_A - \tan\beta$ plane for an integrated luminosity of 100 fb^{-1} .

the electroweak symmetry breaking problem then most of these particles will be in a mass range that is observable at LHC [33] The sparticles with the largest production rates at LHC are those with strong interaction couplings, the squarks and gluinos. Production rates are very large and the discussion then must focus on decay scenarios.

Many supersymmetric models have a discrete symmetry called R-parity that ensures that the lightest supersymmetric particle is absolutely stable. This particle must be electrically neutral and might pervade all of the current universe providing a substantial fraction of the dark matter. This particle could be the partner of the neutrino (sneutrino), but in most supersymmetric models it is one of the four mass eigenstates that are linear combinations the partners of the Z , γ , and neutral components of the two Higgs doublets. These states (in order of increasing mass) are denoted by χ_1 , χ_2 , χ_3 and χ_4 . The production rates for these particles are small and their largest source is the decay of other supersymmetric particles. Since these so-called neutralinos have no electric charge and no strong interactions, they have very small interaction cross-sections off regular matter. The lightest of them exits the detector carrying off energy and leading to one of the classic signals for supersymmetry at a hadron collider: missing E_T .

Heavier neutralinos can decay into lighter ones via the emission of a (real or virtual) Z boson. The partners of the W boson (χ^\pm) can either be produced directly or in the decay of other supersymmetric particles (e.g. $\tilde{g} \rightarrow q\bar{q}\chi^\pm$). The subsequent decay of a χ^\pm will give rise to a (real or virtual) W boson (e.g. $\chi^\pm \rightarrow W\chi_1$) and hence to an isolated leptons. Since the gluino is a Majorana fermion its decay can lead to either ℓ^+ or ℓ^- . This observation leads to the second characteristic signature, Events with one, two or three isolated leptons in various charge combinations. The final state with a pair of isolated leptons of the same charge is particularly interesting as standard model physics (such as the production of a $t\bar{t}$ pair) leads to a rate for this that is much below that for an isolated lepton pair of opposite charge.

The mass spectrum and detailed decay properties of the supersymmetric particles are very model dependent making a general study rather difficult. The situation is complicated by the real possibility that the LHC may be a factory for supersymmetric particles; many different ones are produced at the same time. Early studies of supersymmetric signals concentrated on a specific particle and a particular decay mode demonstrating that cuts could be made that ensure that the signal from this decay stands out above the standard model background. These studies provide a convincing case that supersymmetry could be discovered at the LHC. The next level of work addresses the question of how the masses and couplings of the particles could be determined and the underlying theory constrained. Here one faces the problem that the dominant background for supersymmetry is supersymmetry itself.

So far, direct searches at the Tevatron have excluded the mass range up to $m_{\tilde{g}} = 230$ GeV.[49] With the main injector and 2 fb^{-1} of luminosity, sensitivity will extend up to $m_{\tilde{g}} \sim 300 - 400$ GeV[50], and if we are lucky we might see something. One of the great strengths of the LHC, however, is that it is sensitive

to supersymmetry over the whole mass range over which the theory makes sense (at least as far as electroweak symmetry breaking is concerned), i.e. $m_{\tilde{g}} \lesssim 1 - 1.5$ TeV.

A. Squark and Gluino searches

There are two distinct sources of background for the supersymmetry signatures involving jets and missing E_T . The first is real physics processes involving, for example, jets produced in association with a Z boson that then decays to $\nu\bar{\nu}$. These backgrounds are detector independent and irreducible. Secondly, backgrounds arise from the mismeasurement of multijet jet final states due to imperfections in the detectors. This can happen because of poor jet energy resolution which then allows a jet's energy to be substantially mismeasured resulting in apparent missing E_T , or cracks and dead material which cause energy to be lost. This background, if it proves to be important, can be reduced by rejecting events where the missing E_T vector is closely aligned with one of the jets.

ATLAS conducted a study of the second background. A sample of four and five jet events was produced using exact matrix element calculations interfaced with JETSET 7.4. This method of generation is expected to be more reliable for events with many widely separated jets than that from a showering Monte-Carlo alone. A parameterization of a GEANT based study [51] of the jet response in the potentially troublesome region between the forward and end cap calorimeters was used. The resulting in background is far below that from the irreducible background as is shown in Figure 14

From this figure it can be seen that the completely unrealistic case where all the energy in the region $3.1 < |\eta| < 3.3$ is lost still produces a background that is far below the irreducible background. This study confirms ones done for the SSC[45] that indicate that these reducible backgrounds are unimportant. Figure 14 also shows that at sufficiently large missing E_T , the signal from the decay of squarks and gluinos exceeds that from standard model background sources.

A similar study was carried out by CMS[46]. Here the MSSM was used as implemented in ISASUSY [48]. The following parameters were chosen: $M_{\tilde{g}} = 1500$ GeV, $m_{\tilde{q}} = 1550$ GeV $\mu = -440$ GeV, $\tan\beta = 2$, $m_{\tilde{t}} = 300$ GeV. Events were selected that have a least 4 jets with $E_T > 100$ GeV, one of them was required to have $E_T > 400$ GeV and another to have $E_T > 200$ GeV. The three highest E_T jets have $|\eta| < 1.5$ and the other has $|\eta| < 2.0$, $E_T^{miss} > 600$ GeV, circularity greater than 0.1 and the invariant mass of the jets and the missing E_T is at least 1500 GeV. For this very massive gluino and squark case, 450 events survive these cuts for an integrated luminosity of 10^5 pb^{-1} . There are 90 background events, 58 of which arise from the production of W and Z bosons in association with jets so a signal can be clearly established. Both ATLAS and CMS can discover gluinos up to $m_{\tilde{g}} = 1500$ GeV.

1. Jets and Leptons

ATLAS conducted a simulation of same sign dilepton signals. Here the dominant background arises from $t\bar{t}$ events: $t\bar{t} \rightarrow W(\rightarrow \ell^+)bW\bar{b}(\rightarrow \ell^+\nu c)$. The requirement that both lep-

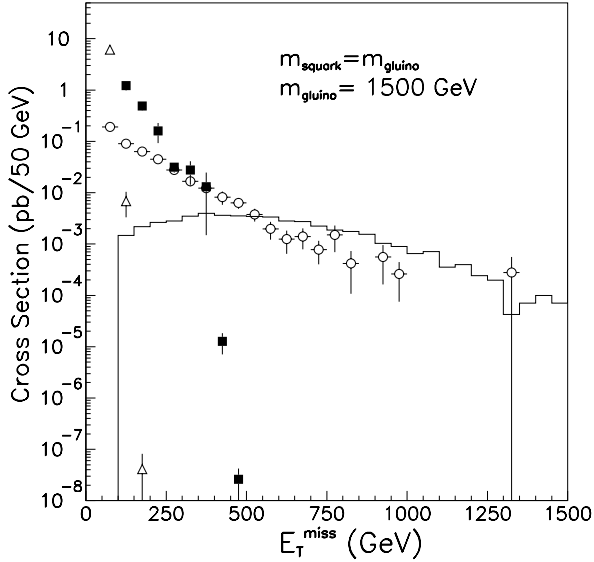


Figure 14: Missing E_T signature arising from a supersymmetry event having at least three jets with $E_T > 200$ GeV, a fourth jet with $E_T > 100$ GeV and transverse sphericity $S_T > 0.2$. The solid histogram is the signal, the open circles are the irreducible background arising from the decay into neutrinos of t , W , Z etc.. The filled squares represent the reducible background in the unreasonable case where all the energy in the region between $|\eta|$ of 3.1 and 3.3 is lost. The more realistic case of degraded resolution is shown as the triangles. Figure from an ATLAS simulation.

tons be isolated (less than 12 (5) GeV of additional energy in a cone of size $\Delta R = 0.2(0.3)$ around the lepton direction at high (low) luminosity), is very effective at reducing the background from bottom decays. Events were required to have two isolated leptons with $p_T > 20$ GeV and $|\eta| < 2.5$, four jets with $E_T > 70(110)$ GeV (at least one of these has $E_T > 110(150)$ GeV) and $E_T^{miss} > 120(150)$ GeV at low (high) luminosity. For an integrated luminosity of 10^5 pb $^{-1}$ and $m_{\tilde{g}} \sim m_{\tilde{q}}$ there are about 14000 (120) signal events over a background of 500 (70) for $m_{\tilde{g}} = 300(1500)$ GeV. The results of this study can be converted into a reach in the MSSM. For most values of $\tan \beta$ and μ , and for $m_{\tilde{g}} \sim m_{\tilde{q}}$ ($m_{\tilde{g}} \sim 2m_{\tilde{q}}$) [$2m_{\tilde{g}} \sim m_{\tilde{q}}$], gluino masses up to 1800 (2600) [1400] GeV can be probed in this channel.

If squark production is dominant, there will be an asymmetry in the signs of the dilepton pairs that arises because the beams are protons which contain more up than down type quarks. This asymmetry is

$$A = \frac{\sigma(++) - \sigma(--)}{\sigma(++) + \sigma(--) + \text{background}}$$

The asymmetry is very small if $m_{squark} = 2m_{gluino}$ but it rises to $A \sim 0.2$ for $m_{squark} = m_{gluino}/2$ and for this value could be measured with a precision of $\delta A = 0.05$ up to squark masses of 750 GeV. This quantity is an example of ones that will be used to pin down the details of the supersymmetry spectrum after a signal has been observed.

CMS have also investigated muon(s)+jets+ E_T signatures for supersymmetry[47]. Channels with a single muon, two muons of the same or of any sign, two isolated muons, and three muons were investigated. These channels are found to allow the observation of a gluino signal up to $m_{gluino} \approx 1.5$ TeV with 10^5 pb $^{-1}$.

B. Charginos and Neutralinos

The pair production of charginos and neutralinos will result in final states with three isolated leptons from the decay chains $\chi^\pm \rightarrow \ell\nu\chi_1$ and $\chi_2 \rightarrow \chi_1\ell^+\ell^-$. After isolation requirements on the leptons, the dominant background is from WZ final states. This final state has been used at the Tevatron. No signal was observed allowing a cross section limit to be set[49].

ATLAS used the MSSM to investigate the utility of this mode at LHC. Three isolated leptons with $|\eta| < 2.5$ were required, two of which have $p_T > 20$ GeV and the third has $p_T > 10$ GeV. Events were rejected if they are had a lepton pair consistent with the decay of a Z (reconstructed mass within 10 GeV of the Z mass). This cut did not reduce the signal because, over the parameter space searched, $m_{\chi_2} - m_{\chi_1} < 80$ GeV. MSSM parameters $\tan \beta = 2$ and 20 , $\mu = -m_{gluino}$, $m_{squark} = 2m_{gluino}$ and $m_{squark} = m_{gluino} + 20$ GeV for $m_{gluino} = 200, 300, 400, 500$ and 600 GeV were used. A jet veto to reduce further the $t\bar{t}$ background was used (no jets with $p_T > 25$ GeV and $|\eta| < 3$) although this cut may not be needed (check this). At low luminosity 10 fb $^{-1}$ (the jet veto is questionable at high luminosity), there is a statistically significant signal up to gluino masses of 600 (400) GeV at the smaller (larger) value of $\tan \beta$.

C. Sleptons

The partners of the leptons are the most difficult supersymmetric particles to observe at a hadron collider. Their production rate is very small as it is dominated by the Drell-Yan process $q\bar{q} \rightarrow \ell^+ \ell^-$, unless sleptons are produced in the decays of strongly interacting sparticles. The slepton decays will produce final states of opposite sign lepton pairs and missing E_T . Backgrounds notably from $t\bar{t}$ final states are very large. All hope of extracting a signal relies on the efficient use of a jet veto. Simulations of slepton signals have not yet been carried out with the ATLAS or CMS detectors. However a ‘‘toy simulation’’ with some degree of credibility indicates that it might be possible to extract a signal[52]. Events were selected requiring that there be a pair of isolated leptons of the same flavor and opposite charge and $p_T > 20$ GeV. At least 100 GeV of missing E_T was required and events were vetoed if there was a jet with $p_T > 25$ GeV and $|\eta| < 3$. The missing E_T vector and the transverse momentum vector of the dilepton system were more than 160° apart in azimuth. The dominant background is from $t\bar{t}$ and W^+W^- events. Slepton masses up to about 300 GeV are observable with 10 fb^{-1} of integrated luminosity. The signal is not obscured by other SUSY decays. This study is very encouraging, a more detailed simulation is required to confirm it. Such investigations are now in progress in CMS, including the question of separating the slepton signal from the backgrounds arising from the copious production of other SUSY states.

D. Which SUSY?

From the studies described above and others one can give absolute confidence that the LHC can discover supersymmetry if it is kinematically accessible. The more difficult question of how well masses and branching ratios can be measured has recently begun to be studied. The proliferation of models makes a systematic approach difficult. In a seminal work, Paige *et al.* have investigated the dependence of the signals discussed above and many others upon the parameters in the minimal supergravity model (SUGRA)[58]. This model has the advantage that rather few parameters specify it completely. The model is assumed to unify at some high scale where a common gaugino mass $m_{1/2}$ is defined. All scalar particles are assumed to have a common mass m_0 at this scale. Three other parameters then fully specify the model: $\tan \beta$, a variable A with dimension of mass that affects mainly the splitting between the partners of the left and right handed top quark, and the sign of μ . Final states involving leptons, jets and missing E_T were investigated to determine sensitivity to the parameters that an LHC experiment may have. One result of this study is that b -quark tagging might be an important tool in disentangling the parameter space as the b -quark multiplicity is a useful quantity to measure.

A study [53] has attempted to address the issue of how well the parameters in a SUGRA model could be determined. The proposed strategy is as follows. One first searches for an excess of events over background by using several variables. For example, events are selected which have at least 4 jets one of which has $E_t > 100$ GeV and the others have $E_T > 50$. An additional requirement of $E_T^{miss} > 100$ GeV and sphericity $S > 2$

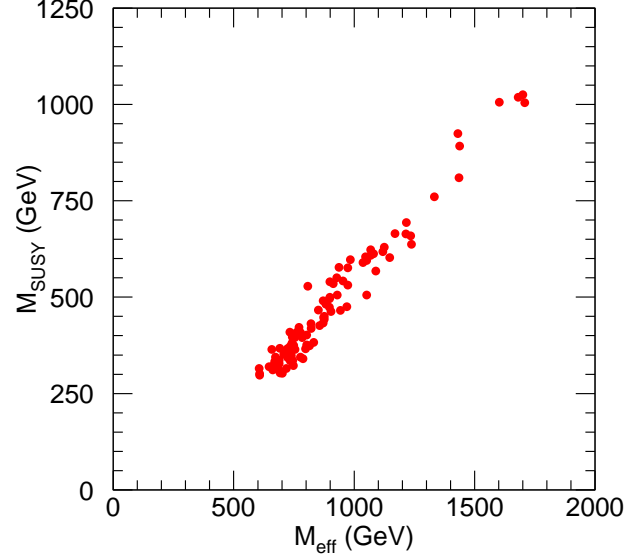


Figure 15: The correlation between the peak in the M_4 distribution, M_{eff} and M_{susy} being the smaller of the gluino and average of the up, down charm and strange squark masses.

is made, and the event rate is plotted against M_4 defined as the scalar sum of the E_T of the four jets and E_T^{miss} [54]. This curve has a peak in the region where the signal to background ratio is large and there is a strong correlation between the position of the peak and the smallest of the gluino and (up, down, strange and charm) squark masses as is shown in Figure 15. This correlation can then be exploited to determine the overall mass scale for the strongly interacting superparticles with an accuracy of order 10%.

Having determined the scale, more detailed measurements are then performed. For this purpose a particular point in the parameter space was selected for simulation. The mass spectrum is as follows: Gluino $m_{\tilde{g}} = 298$ GeV $m_{\tilde{q}_r} = 312$ GeV, $m_{\tilde{q}_l} = 317$ GeV $m_{\tilde{t}_1} = 263$ GeV, $m_{\tilde{t}_2} = 329$ GeV $m_{\tilde{b}_1} = 278$ GeV, $m_{\tilde{b}_2} = 314$ GeV Sleptons $m_{\tilde{e}_l} = 215$ GeV, $m_{\tilde{e}_r} = 206$ GeV, Neutralinos $m_{\chi_1} = 44$ GeV, $m_{\chi_2} = 98$ GeV, $m_{\chi_3} = 257$ GeV, $m_{\chi_4} = 273$ GeV Charginos $m_{\tilde{\chi}_1^+} = 96$ GeV, $m_{\tilde{\chi}_2^+} = 272$ GeV Higgs $m_h = 68$ GeV, $m_H = 378$ GeV, $m_A = 371$ GeV, $m_{H^+} = 378$ GeV.

At this point the total production rate for gluino pairs is very large, and many other supersymmetric particles are produced in the decay of gluinos. Of particular significance is χ_2 which decays to $\chi_1 e^+ e^-$ and $\chi_1 \mu^+ \mu^-$ with a combined branching ratio of 32%. The position of the end point of this spectrum determines the mass difference $m_{\chi_2} - m_{\chi_1}$ [55]. Backgrounds are negligible if the events are required to have two such dilepton pairs, which can arise from the pair production of gluinos with each decaying to $b\bar{b}(\rightarrow \chi_2(\rightarrow \chi_1 \ell^+ \ell^-))$ which has a combined branching ratio of 24%. The event rate is so large that the sta-

tistical error in the determination of the mass difference is very small and the total error will be dominated by systematic effects. The enormous number of $Z \rightarrow \ell^+ \ell^-$ decays can be used to calibrate, and an error of better than 50 MeV on $m_{\chi_2} - m_{\chi_1}$ is achievable³. In the context of the model, this measurement constrains $M_{1/2}$ with an error of order 0.1%. By comparing event rates for samples with one or two dilepton pairs, the branching ratio $\chi_2 \rightarrow \chi_1 \mu^+ \mu^-$ can be measured.

The small mass difference between the gluino and the sbottom can also be exploited to reconstruct the masses of these particles [57]. Here a partial reconstruction technique is used. Events are selected where the dilepton invariant mass is close to its maximum value. In the rest frame of χ_2 , χ_1 is then forced to be at rest. The momentum of χ_2 in the laboratory frame is then related to the momentum of the $\ell^+ \ell^-$ pair by $p_{\chi_2} = (1 + m_{\chi_1}/m_{\ell^+ \ell^-}) p_{\ell^+ \ell^-}$. χ_2 can then be combined with an additional $b - j_{et}$ to reconstruct the $\tilde{t} \tilde{d} b$ mass. An additional $b_j et$ can then be added to reconstruct the \tilde{g} mass. Figure 16 shows the scatterplot on these two invariant masses together with a projection onto $m_{\tilde{b}}$ and $\delta m = m_{\tilde{t} \tilde{d} e g} - m_{\tilde{b}}$. Peaks can clearly be seen above the combinatoric background. This method can be used to determine $m_{\tilde{g}}$ and $m_{\tilde{b}}$. The values depend on the assumed value of m_{χ_1} : $m_{\tilde{b}} = m_b^{true} + 1.5(m_{\chi_1}^{assumed} - m_{\chi_1}^{true}) \pm 3 \text{ GeV}$ and $m_{\tilde{g}} - m_{\tilde{b}} = m_{\tilde{g}}^{true} - m_b^{true} \pm 0.5 \text{ GeV}$.

Once several quantities have been measured, one will attempt to constrain the parameters of the SUSY model by performing a global fit much as the standard model is tested at LEP [60]. To get an indication of how well this might work, many choices of parameters within the SUGRA model were made and those that resulted in masses within the expected error were retained [53]. Measurements of m_h , $m_{\chi_2} - m_{\chi_1}$ and $m_{\tilde{g}} - m_{\tilde{b}}$ with errors of $\pm 5 \text{ GeV}$, $\pm 0.50 \text{ GeV}$ (10σ) and $\pm 3 \text{ GeV}$ (1.5σ) respectively result in the constraints $\delta m_{1/2} = 1.5 \text{ GeV}$, $\delta m_0 = 15 \text{ GeV}$ and $\delta \tan \beta = 0.1$. It is clear from this example that precise measurements of SUSY parameters will be made at LHC if supersymmetric particles exist.

Other supersymmetric models such as the recently popular models where supersymmetry is broken at a rather low scale [61], can produce signals different from SUGRA models. In particular χ_1 may be unstable and may decay to $\gamma + \tilde{G}$, reducing the missing E_T rate (\tilde{G} exits unobserved) but providing every supersymmetry event with an additional pair of isolated photons. We should hope that these models are correct as this signal is trivial to observe at LHC.

V. Strong Dynamics

A. Strongly interacting W 's

The couplings of longitudinally polarized gauge bosons to each other are fixed at low energy by the nature of the spontaneously broken electro-weak symmetry and are independent of the details of the breaking mechanism. Scattering amplitudes calculated from these couplings will violate unitarity at center of

³Recall that the current error on M_W from CDF/D0 [56] comes from an analysis involving E_T^{miss} has far fewer events and has an error of order 150 MeV

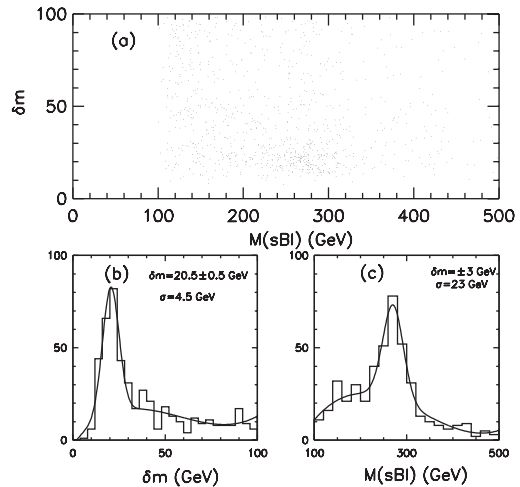


Figure 16: The reconstruction of gluino and sbottom decays from the decay chain $\tilde{g} \rightarrow \chi_2 (\rightarrow \chi_1 \ell^+ \ell^-) \tilde{b}$. Events are selected near the end point of the $\ell^- \ell^+$ mass distribution and the momentum of χ_2 is reconstructed. Two b -jets are then required and the mass of $b + \chi_2$ ($= m_{\tilde{b}}$) and the mass difference $\delta m = m_{b b \chi_2} - m_{b \chi_2}$ are computed. The scatterplot in these two variables and the projections are shown.

mass energies of the WW system around 1.5 TeV. New physics must enter to cure this problem. In the minimal standard model and its supersymmetric version, the cure arises from the perturbative couplings of the Higgs bosons. If no Higgs-like particle exists, then new non-perturbative dynamics must enter in the scattering amplitudes for WW , WZ and ZZ scattering at high energy. Therefore if no new physics shows up at lower mass scales one must be able to probe $W_L W_L$ scattering at $\sqrt{s} \sim 1 \text{ TeV}$.

Various models exist that can be used as benchmarks for this physics [63]. The basic signal in all of them is an excess of events over that predicted by the standard model for gauge boson pairs of large invariant mass. In certain models resonant structure can be seen (an example of this is given in the next subsection). In the standard model, the $W^+ W^+$ final state is the only one where there is no process $q\bar{q} \rightarrow WW$ and is therefore expected to have a much smaller background than, for example, the ZZ or $W^+ W^-$ final state. Background is present at a smaller level from $q\bar{q} \rightarrow W q\bar{q}$ proceeding either by gluon

exchange or via an order α^2 electroweak process and from the final state $Wt\bar{t}$. There is a background from WZ if one lepton is lost. There is negligible background from charge misidentification in either ATLAS or CMS.

ATLAS [64] conducted a parton model study of the signal and background in this channel. Events were selected that have two leptons of the same sign with $p_T > 25$ GeV and $|\eta| < 2.5$. If a third lepton was present that, in combination with one of the other two, was consistent with the decay of a Z (mass within 15 GeV of the Z mass), the event was rejected. This cut is needed to eliminate the background from WZ and ZZ final states. In addition the two leptons are required to have invariant mass above 100 GeV, to have transverse momenta within 80 GeV of each other and to be separated in ϕ by at least $\pi/2$. At this stage, there are there are ~ 1700 standard model events for a luminosity of 10^5 pb $^{-1}$. Of these events roughly 50% are from WZ and ZZ final states and 30% from $Wt\bar{t}$. There are of order 40 signal events depending upon the model used for the strongly coupled gauge boson sector. Additional cuts are needed to reduce the background. A jet veto requiring no jets with $p_T > 40$ GeV and $|\eta| < 2$ is effective against the $Wt\bar{t}$ final state. The requirement of two forward jet tags each with $15 < p_T < 130$ GeV and $|\eta| > 3$ reduces the WW , ZZ and WZ background.

The remaining background of 40 events is dominated by the $q\bar{q} \rightarrow Wq\bar{q}$ processes. The signal rates vary between 40 and 15 events depending upon the model. The largest rate arises from a model where the WW scattering amplitude, which is known at small values of \sqrt{s} from low energy theorems is extrapolated until it saturates unitarity and its growth is then cut off. A model assuming that the dynamics of WW scattering is similar to that of $\pi\pi$ scattering in QCD generates approximately 25 signal events. The case of a 1 TeV standard model higgs boson is shown in Fig. 17. It can be seen that the signal and background have the same shape and therefore the establishment of a signal requires confidence in the expected level of the background. The experiment is very difficult, but at full luminosity, a signal might be extracted by comparing the rate for W^+W^+ with those for WZ , W^+W^- , and ZZ final states.

A similar study in CMS of the W^+W^+ final state leads to similar conclusion [68]. Jet tagging (vetoing) in the forward (central) region is essential to extract a signal.

B. Technicolor

Many models of strong electroweak symmetry breaking (technicolor, topcolor-assisted technicolor, BESS [69]) predict resonances which decay into vector bosons (or their longitudinal components). These signals are very striking since they are produced with large cross sections and may be observed in the leptonic decay modes of the W and Z where the backgrounds are very small.

ATLAS have studied a techni-rho, $\rho_T \rightarrow WZ$, with $W \rightarrow \ell\nu$, $Z \rightarrow \ell\ell$, for $m_{\rho_T} = 1.0$ TeV and also a techni-omega, $\omega_T \rightarrow Z\gamma$, with $Z \rightarrow \ell\ell$, for $m_{\omega_T} = 1.46$ TeV. The backgrounds due to $t\bar{t}$ and continuum vector-boson pair production are small as can be seen in Fig.18.

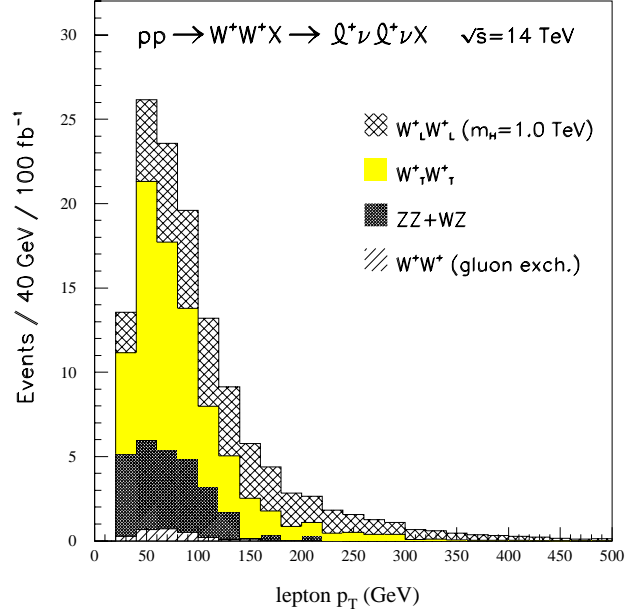


Figure 17: The p_T spectrum for same sign dileptons in the search for a strongly coupled WW sector as simulated by ATLAS. The signal corresponds to a 1 TeV Higgs boson.

More challenging are the possible decays into non-leptonic modes such as $\rho_T \rightarrow W(\ell\nu)\pi_T(b\bar{b})$, which has a signature like associated WH production with $H \rightarrow b\bar{b}$; $\eta_T \rightarrow t\bar{t}$, for which the signature is a resonance in the $t\bar{t}$ invariant mass; and $\rho_{T8} \rightarrow \text{jet jet}$, for which the signature is a resonance in the dijet invariant mass distribution.

C. Compositeness

There is no *a priori* reason for quarks to be elementary. If they have substructure it will be revealed in the deviations of the jet cross-section from that predicted by QCD. The deviation is parameterized by an interaction of the form $4\pi q\gamma^\mu \bar{q}q\gamma^\mu \bar{q}/\Lambda^2$, which has a scale Λ . This is regarded as an effective interaction which is valid only for energies less than Λ . The ATLAS collaboration has investigated the possibilities for searching for structure in the jet cross-section at high p_T . Figure V.C. shows the normalized jet cross section $d\sigma/dp_T d\eta$ at $\eta = 0$. The rate is shown as a function of p_T for various values of Λ and is normalized to the value expected from QCD. The error bars at two values of p_T indicate the size of the statistical error to be expected at that value for luminosities of 10^4 and 10^5 pb $^{-1}$. It can be seen that the LHC at full luminosity will be able to probe up to $\Lambda = 20$ TeV if the systematic errors are smaller than the statistical ones. Systematic effects are of two types; theoretical uncertainties in calculating the QCD rates and detector effects. The former are dependent upon an accurate knowledge of the structure functions in the x range of interest and upon higher order QCD corrections to the jet cross-sections. Uncertainties from these sources can be expected at the 10% level.

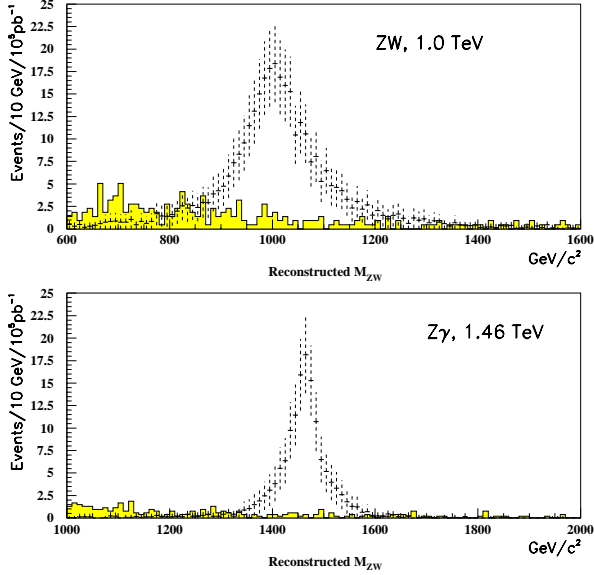


Figure 18: Reconstructed masses for high-mass resonances decaying into gauge boson pairs simulated by ATLAS: (a) ρ_T of mass 1.0 TeV decaying into WZ and subsequently into 3 leptons; and (b) ω_T of mass 1.46 TeV decaying into $Z\gamma$ with $Z \rightarrow 2$ leptons.

Experimental effects are of two types. Mismeasurement due to resolution and nonlinearities in the detector response. The former are at the 20% level; the latter can be more serious and can induce changes in the apparent shape of the jet cross-section. A non-linearity at the 4% level will fake a compositeness signal corresponding to $\Lambda \sim 15$ TeV. Other distributions, such as the angular distribution of the jets in a dijet event selected so that the dijet pair has a very large mass, may be less sensitive to the non-linearities.

A better reach in Λ may be obtained from Drell-Yan dilepton final states, if leptons are also composite.

VI. New Gauge Bosons

A generic prediction of superstring theories is the existence of additional $U(1)$ gauge groups. There is thus motivation to search for additional W' and Z' bosons. The current Tevatron limit is 720 GeV for W' ($D\bar{O}$)[70].

ATLAS have studied the sensitivity to a new neutral Z' boson in e^+e^- , $\mu\mu$ and jet-jet final states, for various masses and couplings[71]. It is assumed that $\Gamma_{Z'} \propto m_{Z'}$. They find the best sensitivity in the ee mode, in which signals could be seen up to $m_{Z'} = 5$ TeV for standard-model couplings. The other final states would provide important information on the Z' couplings. The pseudorapidity coverage over which lepton identification and measurement can be carried out is important for Z' searches: should a signal be observed, the forward-backward asymmetry of the charged leptons would provide important in-

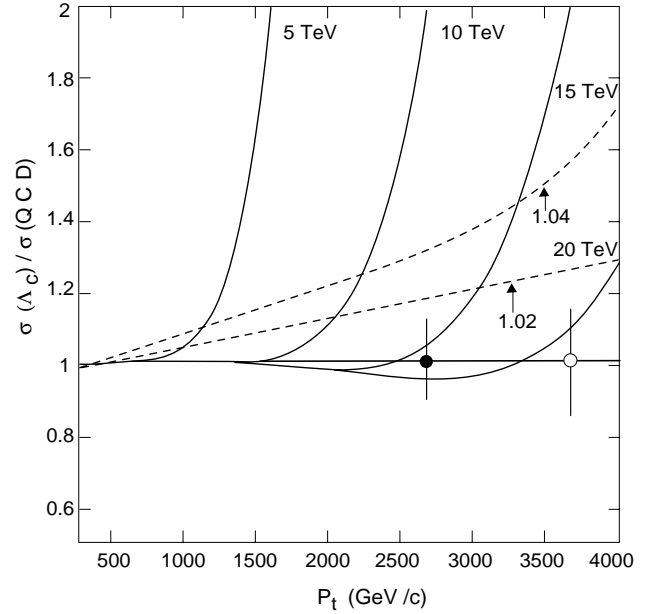


Figure 19: Deviation from QCD for various values of the compositeness scale Λ . The error bars correspond to statistical sensitivities at 100 fb^{-1} (open circle) and 10 fb^{-1} . The dotted lines refer to the errors induced by possible nonlinearities in the ATLAS calorimeter.

formation on its nature. ATLAS found that reducing the lepton coverage from $|\eta| \leq 2.5$ to $|\eta| \leq 1.2$ roughly halved the observed asymmetries and prevented discrimination between two particular Z' models which they investigated.

ATLAS also investigated their sensitivity to a new charged boson W' decaying into $e\nu$. The signal is structure in the transverse mass distribution at masses much greater than m_W . Figure 17 shows the signal for a 4 TeV W' . They conclude that with 10^5 pb^{-1} one would be sensitive to $m_{W'} = 6$ TeV and that the mass could be measured to 50–100 GeV.

VII. Anomalous Gauge-Boson Couplings

The trilinear WWV and $Z\gamma V$ couplings ($V = Z, \gamma$) may be probed at hadron colliders using diboson final states. Following the usual notation, the CP-conserving WWV anomalous couplings are parameterized in terms of $\Delta\kappa_V$ and λ_V , where $\kappa_V = 1$ and $\lambda_V = 0$ in the Standard Model for $V = Z, \gamma$. In general, we would expect anomalous couplings of order m_W^2/Λ^2 if Λ is the scale for new physics, so if $\Lambda \sim 1$ TeV then $\Delta\kappa_V, \lambda_V \sim 0.01$. The $Z\gamma V$ anomalous couplings are parameterized in terms of h_3^V and h_4^V , where $h_3^V = h_4^V = 0$ in the Standard Model and deviations are expected to be $\mathcal{O}(m_W^4/\Lambda^4)$.

To maintain unitarity, the observed anomalous couplings must be modified by a form factor; so (for example)

$$\Delta\kappa_V(q^2) = \frac{\Delta\kappa_V^0}{(1 + q^2/\Lambda_{FF}^2)^n} \quad (1)$$

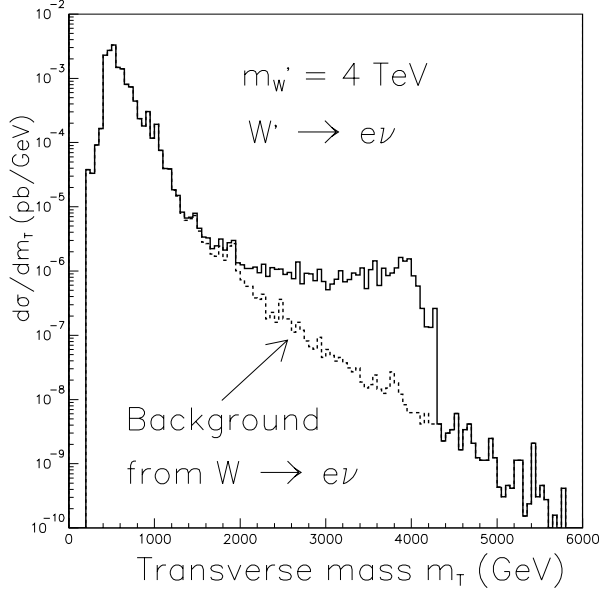


Figure 20: Expected electron-neutrino transverse mass distribution in ATLAS for $W' \rightarrow e\nu$ decays with $m_{W'} = 4$ TeV above the dominant background from $W \rightarrow e\nu$ decays.

where Λ_{FF} is the form factor scale and $n = 2$ for $\Delta\kappa_\gamma, \lambda$ and $n = 3, 4$ for h_3^V, h_4^V .

The ATLAS collaboration have studied[65] their sensitivity to anomalous couplings in the $W\gamma$ and WZ modes; the W^+W^- signal is swamped by $t\bar{t}$ background. A form factor scale $\Lambda_{FF} = 10$ TeV was used. For the $W\gamma$ final state, events were assumed to be triggered using a high- p_T lepton plus high- p_T photon candidate. The background includes contributions from events with a real lepton and a real photon (e.g. $b\bar{b}\gamma, t\bar{t}\gamma,$ and $Z\gamma$); a fake lepton but a real photon (e.g. $\gamma + \text{jet}$); and a fake photon with a real lepton (e.g. $W + \text{jet}, b\bar{b},$ and $t\bar{t}$). Rejection factors of 10^4 against jets faking photons and 10^5 against jets faking electrons were assumed. To reduce backgrounds, events were selected with $p_T^\gamma > 100$ GeV/c, $p_T^\ell > 40$ GeV/c, and $|\eta^\ell| < 2.5$. Events with jets were also vetoed, to further reduce backgrounds and to lessen the importance of higher-order QCD corrections. In an integrated luminosity of 10^5 pb $^{-1}$, 7500 events remain, with a signal to background ratio of 3:1. The p_T^γ distribution is then fitted in the region where the standard model prediction is 15 events (above about 600 GeV/c), yielding limits of $|\Delta\kappa_\gamma| < 0.04$ and $|\lambda_\gamma| < 0.0025$ (95% C.L.).

Similar techniques were used for the WZ state. The trigger was three high- p_T leptons, and the backgrounds are from $Zb\bar{b}, Z + \text{jet}, b\bar{b}$ and $t\bar{t}$ processes. Events were selected with $p_T^\ell > 25$ GeV/c, $|\eta^\ell| < 2.5$, $|m_{\ell_1\ell_2} - m_Z| < 10$ GeV/c 2 , and $m_T(\ell^3, E_T^{miss}) > 40$ GeV/c 2 ; a jet veto was also imposed. In 10^5 pb $^{-1}$, 4000 events then remain, with a signal to background ratio of 2:1. The p_T^Z distribution is again fitted in the region where the standard model prediction is 15 events (above about

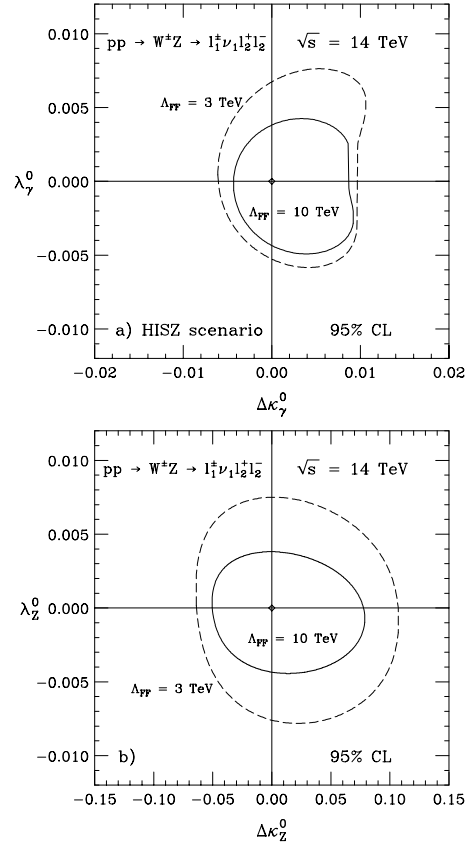


Figure 21: 95% CL sensitivity limits from $W^\pm Z \rightarrow \ell_1^\pm \nu_1 \ell_2^+ \ell_2^-$ at the LHC (a) in the HISZ scenario and (b) if only $\Delta\kappa_Z$ and λ_Z are allowed to deviate from the Standard Model.

380 GeV/c), yielding limits of $|\Delta\kappa_Z| < 0.07$ and $|\lambda_Z| < 0.005$ (95% C.L.).

Studies[66] have also been carried out for the 1994 DPF Long Range Planning Workshop. For WZ states, the $ee\ell\nu$ signal only was considered, and it was required that $p_T^\ell > 25$ GeV/c, and $E_T^{miss} > 50$ GeV. A binned likelihood fit to the p_T^Z distribution then yields limits on $\Delta\kappa_Z$ and λ_Z which are shown in Fig21. For $W\gamma$ and $Z\gamma$ states, a combination of ATLAS resolutions and CDF efficiencies was assumed. It was required that $p_T^\ell > 40$ GeV/c, $p_T^\gamma > 25$ GeV/c, $E_T^{miss} > 25$ GeV ($W\gamma$ only), and $m(\ell\ell\gamma) > 110$ GeV/c 2 ($Z\gamma$ only). A separation of $\Delta R > 0.7$ between the lepton and photon was required, and events with any jet with E_T above 50 GeV were vetoed. A binned likelihood fit to the p_T^γ distributions then yields limits on $\Delta\kappa_\gamma, \lambda_\gamma, h_3^Z$ and h_4^Z which are shown in Fig22.

The limits obtained in all the above studies are summarized in Table II. It will be possible to probe WWV anomalous couplings with a precision of order $10^{-1} - 10^{-3}$ if the form factor scale $\Lambda_{FF} > 2$ TeV. This is sufficient to just reach the interesting region where one may hope to see deviations from the standard model given present limits on the scale of new physics.

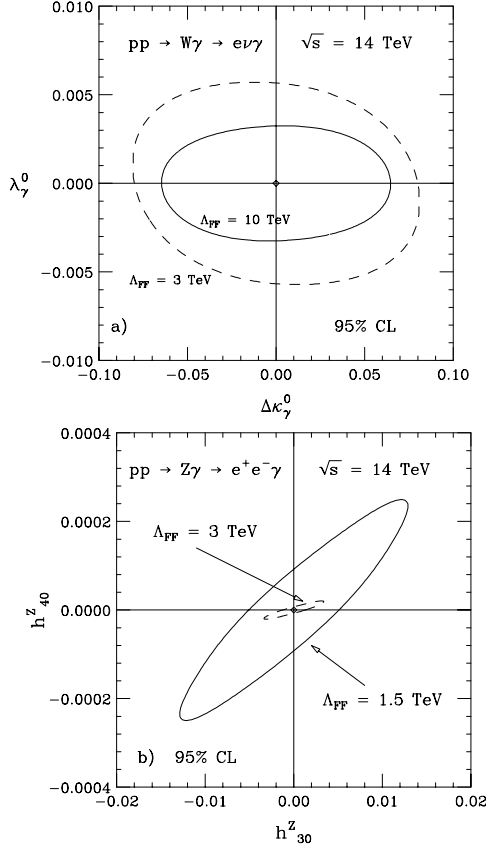


Figure 22: 95% CL sensitivity limits for (a) $WW\gamma$ couplings from $W\gamma$ production and (b) $ZZ\gamma$ couplings from $Z\gamma$ production at the LHC. Results are displayed for an integrated luminosity of 100 fb^{-1} and two different form factor scales.

VIII. Standard Model Physics

A. Top Quark Physics

The potential for the study of the top quark at hadron colliders is already apparent. Its recent discovery at the Tevatron undoubtedly presages a long and fruitful program of top physics studies. The LHC will be a top factory, with about 10^7 $t\bar{t}$ pairs produced per year at a luminosity of $10^{33} \text{ cm}^{-2} \text{ s}^{-1}$. This would result in about 200,000 reconstructed $t\bar{t} \rightarrow (\ell\nu b)(j\bar{j}b)$ events and 20,000 clean $e\mu$ events.

1. Top Mass Measurement

The top mass may be reconstructed from the $t\bar{t} \rightarrow (\ell\nu b)(j\bar{j}b)$ final state using the invariant mass of the 3-jet system. Problems arise from the presence of backgrounds, from combinatorics, and from systematic effects due to the detector and the theoretical models used. ATLAS[1] have estimated that an accuracy of ± 3 GeV could be attained. By selecting very high- p_T top quarks, where the decay products are boosted and thus close, combinatorics may be reduced, and the mass measured to perhaps ± 2 GeV. This measurement requires, of course, that the

Channel	Study	Limit
$pp \rightarrow W^\pm \gamma \rightarrow e^\pm \nu \gamma$	DPF ATLAS	$\Lambda_{FF} = 3 \text{ TeV}$: $ \Delta\kappa_\gamma^0 < 0.080$ $ \lambda_\gamma^0 < 0.0057$ $\Lambda_{FF} = 10 \text{ TeV}$: $ \Delta\kappa_\gamma^0 < 0.065$ $ \lambda_\gamma^0 < 0.0032$ $\Lambda_{FF} = 10 \text{ TeV}$: $ \Delta\kappa_\gamma^0 < 0.04$ $ \lambda_\gamma^0 < 0.0025$
$pp \rightarrow W^\pm Z \rightarrow \ell\nu\ell\ell$ $\ell = e, \mu, \text{ HISZ [67]}$	DPF	$\Lambda_{FF} = 3 \text{ TeV}$: $-0.0060 < \Delta\kappa_\gamma^0 < 0.0097$ $-0.0053 < \lambda_\gamma^0 < 0.0067$ $\Lambda_{FF} = 10 \text{ TeV}$: $-0.0043 < \Delta\kappa_\gamma^0 < 0.0086$ $-0.0043 < \lambda_\gamma^0 < 0.0038$
$pp \rightarrow W^\pm Z \rightarrow \ell\nu\ell\ell$ $\ell = e, \mu, \Delta g_1^Z = 0$	DPF ATLAS	$\Lambda_{FF} = 3 \text{ TeV}$: $-0.064 < \Delta\kappa_Z^0 < 0.107$ $-0.0076 < \lambda_Z^0 < 0.0075$ $\Lambda_{FF} = 10 \text{ TeV}$: $-0.050 < \Delta\kappa_Z^0 < 0.078$ $-0.0043 < \lambda_Z^0 < 0.0038$ $\Lambda_{FF} = 10 \text{ TeV}$: $ \Delta\kappa_Z^0 < 0.07$ $ \lambda_Z^0 < 0.005$
$pp \rightarrow Z\gamma \rightarrow e^+e^-\gamma$	DPF	$\Lambda_{FF} = 1.5 \text{ TeV}$: $ h_{30}^Z < 0.0051$ $ h_{40}^Z < 9.2 \cdot 10^{-5}$ $\Lambda_{FF} = 3 \text{ TeV}$: $ h_{30}^Z < 0.0013$ $ h_{40}^Z < 6.8 \cdot 10^{-6}$

Table II: Expected 95% CL limits on anomalous WWV , $V = \gamma, Z$, and $ZZ\gamma$ couplings from experiments at the LHC. Only one of the independent couplings is assumed to deviate from the SM at a time. The limits obtained for $Z\gamma\gamma$ couplings almost coincide with those found for h_3^Z and h_4^Z .

hadronic calorimetry be calibrated to this level in the absolute energy scale and that its response be stable over time. CMS have investigated the possibility of in-situ calibration of the jet response within top events by reconstruction of the hadronic W decays, a possibility already evident in the present CDF and $D\Phi$ data.

The mass may also be reconstructed from dilepton events. ATLAS estimate that, by selecting events with two leptons from W decays and an additional lepton from b -decay, and plotting the invariant mass of the lepton pair originating from the same top decay, the mass could be determined with a statistical accuracy of ± 0.5 GeV, and a total accuracy of about ± 2 GeV. The dominant systematic errors arise from uncertainties in the b -quark fragmentation and are therefore complementary to the 3-jet system which is dominated by calorimeter and jet systematics.

1. Search for Charged Higgs

In extensions of the standard model with charged higgs bosons H^\pm , such as in the MSSM, the decay $t \rightarrow bH^\pm$ may compete with the standard $t \rightarrow bW^\pm$ if kinematically allowed. The H^\pm decays to $\tau\nu$ or $c\bar{s}$ depending on the value of $\tan\beta$. Over most of the range $1 < \tan\beta < 50$, the decay mode $H^\pm \rightarrow \tau\nu$ dominates. The signal for H^\pm production is thus an excess of taus produced in $t\bar{t}$ events.

Both ATLAS[72] and CMS[73] have investigated the sensitivity to this excess. Top events with at least one isolated high- p_T lepton are selected, and the number having an additional tau compared with the number having an additional e or μ . Both studies used b -tagging to reduce the backgrounds to top production. Taus were identified in a way very similar to that described earlier (in the section on $A, H \rightarrow \tau\tau$ searches). The uncertainty in the tau excess is estimated to be $\pm 3\%$, dominated by systematics. For an integrated luminosity of 10^4 pb^{-1} , both ATLAS and CMS conclude that over most of the $\tan\beta$ range, a signal can be observed at the 5σ level for $m_{H^\pm} < 130 \text{ GeV}$, which corresponds to the region $m_A \lesssim 120 \text{ GeV}$ in the $m_A, \tan\beta$ plane.

1. Rare Top Decays

The large statistics available at LHC will provide sensitivity to other non-standard or rare top decays. As an example, ATLAS have investigated the channel $t \rightarrow Zc[1]$, which should occur at a negligible level in the SM. With an integrated luminosity of 10^5 pb^{-1} , branching ratios as small as 5×10^{-5} could be measured.

The TeV2000 study[50] estimates that LHC will attain a precision 2–3 times better than TeV33 on the ratio of longitudinal to left-handed W 's produced in t decays. This ratio is exactly predicted in the SM for a given top mass, and is sensitive to non-standard couplings at the $t \rightarrow Wb$ vertex, such as a possible $V + A$ contribution.

B. b Physics

The preceding sections have shown the importance of b -tagging in addressing many of the high- p_T physics goals of the LHC. Both major detectors will consequently have the capability to tag heavy flavor production through displaced vertices. This capability, together with the b -quark production cross-section at the LHC, will enable them to also pursue a targeted but interesting program of b -physics. It can be assumed that CP violation in the b -quark system will have been observed before the LHC gives data. Nevertheless the enormous rate will enable a very precise determination of $\sin 2\beta$ to be made using the decay $B_u \rightarrow \psi K_S$. An error of ± 0.02 can be expected after 10 fb^{-1} of integrated luminosity. It should also be possible to measure $B_s \bar{B}_s$ mixing and to search for rare decays such as $B \rightarrow \mu\mu$.

IX. Summary and Conclusions

The LHC is unique among accelerators currently existing or under construction. It will have sufficient energy and luminos-

ity to enable vital discoveries to be made and will lead to insight into the mass generation mechanism of the standard model. The very detailed simulation studies carried out by the ATLAS and CMS collaborations enable one to make the following statements with a high degree of confidence:-

- If the minimal standard model is correct and the higgs boson is not discovered at LEP II, it will be found at LHC.
- If supersymmetry is relevant to the breaking of electroweak symmetry, it will be discovered at LHC and many details of the particular supersymmetric model will be disentangled.
- If the Higgs sector is that of the minimal supersymmetric model, at least one Higgs decay channel will be seen, no matter what the parameters turn out to be. In many cases, several Higgs bosons or decay channels will be seen.
- If the electroweak symmetry breaking proceeds via some new strong interactions, many resonances and new exotic particles will almost certainly be observed.
- New gauge bosons with masses less than several TeV will be discovered or ruled out.

A great opportunity and a vast amount of excitement is promised to those physicists fortunate enough to be part of an LHC experiment.

REFERENCES

- [1] Atlas Technical proposal, CERN/LHCC/94-43.
- [2] CMS Technical proposal, CERN/LHCC/94-38.
- [3] M. Kobayashi, T. Maskawa, *Prog. Theor. Phys.* 49:652 (1973). N. Cabibbo,
- [4] K. Arisaka, *et al.*, FERMILAB-FN-580 (1992).
- [5] D. Boutigny, *et al.*, SLAC-R-95-457, M.T. Cheng, *et al.*, KEK Report BELLE-TDR-3-95.
- [6] S. Glashow, *Nucl. Phys.* **22**, 579 (1961); S. Weinberg, *Phys. Rev. Lett.* **19**, 1264 (1967); A. Salam, in: "Elementary Particle Theory," W. Svartholm, ed., Almquist and Wiksell, Stockholm (1968); H.D. Politzer, *Phys. Rev. Lett.* **30**, 1346 (1973); D.J. Gross and F.E. Wilczek, *Phys. Rev. Lett.* **30**, 1343 (1973).
- [7] G. Miller, *et al.*, *Phys. Rev.* **D5**, 6528 (1972), A. Bodek, *et al.*, *Phys. Rev. Lett.* **30**, 1087 (1973).
- [8] J.J. Aubert, *et al.*, *Phys. Rev. Lett.* **33**, 1404 (1974); J.E. Augustin, *et al.*, *Phys. Rev. Lett.* **33**, 1406 (1974); G. Goldhaber, *et al.*, *Phys. Rev. Lett.* **37**, 255 (1976); S.W. Herb, *et al.*, *Phys. Rev. Lett.* **39**, 252 (1977); D. Andrews, *et al.*, *Phys. Rev. Lett.* **45**, 219 (1980).
- [9] F.J. Hasert, *et al.*, *Phys. Lett.* **46B**, 138 (1973).
- [10] R. Brandelik, *et al.*, *Phys. Lett.* **86B**, 243 (1979); D.P. Barber, *et al.*, *Phys. Rev. Lett.* **43**, 830 (1979); C. Berger, *et al.*, *Phys. Lett.* **86B**, 418 (1979); W. Bartel, *et al.*, *Phys. Lett.* **91B**, 142 (1980).
- [11] F. Abe *et al.* *Phys. Rev. Lett.* **73**, 2667 (1994), *Phys. Rev.* **D52**, 2605 (1995); S. Abachi *et al.* *Phys. Rev. Lett.* **74**, 2632 (1995).

- [12] G. Arnison, *et al. Phys. Lett.* **126B**, 398 (1983), G. Arnison, *et al. Phys. Lett.* **122B**, 103 (1983).
- [13] For example see, L Wolfenstein, hep-ph/9604389.
- [14] R.N. Cahn, R. N., LBL-38649 (1996), submitted to *Rev. Mod. Phys.*
- [15] C. Quigg, B.W. Lee and H. Thacker, *Phys. Rev.* **D16**, 1519 (1977) M. Veltman, *Acta Phys. Polon.* B8:475 (1977).
- [16] For a review see, I. Hinchliffe, *Ann. Rev. Nucl. and Part. Sci.* **36**, 505 (1986);
- [17] For a review see, K.D. Lane hep-9605257 (1996).
- [18] P. Lefevre, *et al.*, CERN/AC/95-05.
- [19] ALICE Technical Proposal, CERN/LHCC/95-71.
- [20] LHC-B Technical Proposal, CERN/LHCC/95-XX.
- [21] E. Eichten, *et al.*, *Rev. Mod. Phys.* **56**, 579 (1984).
- [22] CERN Program Library, GEANT.
- [23] Review of Particle Properties, *Phys. Rev.* **D54**, 1 (1996).
- [24] LEP report, CERN 96-01.
- [25] C. Seez, CMS-TN/94-289 (1994).
- [26] D. Froidevaux, F. Gianotti and E. Richter Was, ATLAS Note PHYS-NO-064 (1995), F. Gianotti and I. Vichon, ATLAS Note PHYS-NO-078 (1996).
- [27] L. Feyard and G Unal, EAGLE PHYS-NO- 01.
- [28] D. Froidevaux and E. Richer-Was, *Zeit. fur Physik* **C67**, 213 (1995)
- [29] S Haywood, ATLAS internal note INDET-NO-92 (1995), I Gravelenko, *et al.* ATLAS internal note INDET-NO-115 (1995).
- [30] F. Abe, *et al.*, *Phys. Rev.* **D51**, 4623 (191995).
- [31] D. Denegri, R. Kinnunen and G. Roulet, CMS-TN/93-101 (1993).
- [32] J.-C. Chollet, *et al.*, ATLAS internal note PHYS-NO-17 (1992), L. Poggioli, ATLAS Note PHYS-NO-066 (1995).
- [33] Greg W. Anderson, Diego J. Castano *Phys. Rev.* **D53**, 2403 (1996).
- [34] M. Bosman and M. Nessi, ATLAS Note PHYS-NO-050 (1994).
- [35] N.Stepanov, CMS-TN/93-87 (1993); S. Abdullin and N. Stepanov, CMS-TN/94-179 (1994).
- [36] S. Abdullin and N. Stepanov, CMS-TN/94-178 (1994).
- [37] J. Ohnemus, *Phys. Rev.* **D50**, 1931 (1994).
- [38] S. Zmushko, *et al.*, ATLAS Note PHYS-NO-008 (1992).
- [39] M. Carena, M. Quiros, C.E.M. Wagner, *Nucl. Phys.* **B461**, 407 (1996).
- [40] S. Abdullin, C. Kao and N. Stepanov, University of Rochester UR-1475, July 1996.
- [41] R. Kinnunen, J. Tuominiemi, and D. Denegri, CMS-TN/93-98 (1993) and CMS-TN/93-103; C. Seez, CMS-TN/93-84.
- [42] D. Cavalli, *et al.*, ATLAS Note PHYS-NO-025 (1993).
- [43] E. Richer-Was, *et al.*, ATLAS Note PHYS-NO-074 (1996).
- [44] N. Stepanov, CMS-TN/94-182 (1994).
- [45] R.M. Barnett and I. Hinchliffe LBL-28773 (1990).
- [46] M. Greiter, CMS-TN/94-319 (1994); I.Iashvili *et al.*, CMS-TN/93-74 (1993).
- [47] L. Rurua and N.Stepanov, CMS-TN/94-203 (1994); L. Rurua, CMS-TN/94-207 (1994).
- [48] F. Paige and S. Protopopescu, ISAJET V5.04.
- [49] F. Abe, *et al. Phys. Rev. Lett.* **75**, 613 (1995), *Phys. Rev. Lett.* **76**, 2006 (1996); S. Abachi *et al. Phys. Rev. Lett.* **75**, 618 (1995), *Phys. Rev. Lett.* **75**, 613 (191995).
- [50] 'Report of the TeV2000 Study Group on Future Electroweak Physics at the Tevatron,' D. Amidei and R. Brock (eds.), Fermilab 1996.
- [51] A. Artamonov ATLAS internal note CALNO-065 (1994),
- [52] H. Baer, *et al.*, *Phys. Rev.* **D49**, 3283 (1994).
- [53] A. Bartl, *et al.*, To appear in Proceedings of 1996 DPF Summer study; I. Hinchliffe *et al.*, hep-ph/9610544.
- [54] F. Paige, To appear in Proceedings of 1996 DPF Summer study.
- [55] J. Soderqvist, To appear in Proceedings of 1996 DPF Summer study.
- [56] F. Abe, *et al.*, *Phys. Rev. Lett.* **75**, 11 (1995), S. Abachi, *et al.* FERMILAB-PUB-96-177-E.
- [57] W-M Yao, To appear in Proceedings of 1996 DPF Summer study.
- [58] H. Baer, *et al.*, *Phys. Rev.* **D52**, 2746 (1995), *Phys. Rev.* **D51**, 1046 (1995).
- [59] F. Paige, ATLAS Note PHYS-NO-085 (1996).
- [60] LEP Electroweak working group.
- [61] M. Dine, A. Nelson and Y. Shirman, *Phys. Rev.* **D51**, 1362 (1995).
- [62] S Dimopoulos, *et al.*, SLAC-PUB- 96-7104.
- [63] M.S. Chanowitz and M.K. Gaillard, *Nucl. Phys.* **B261**, 379 (1985).
- [64] G. Azuelos, *et al.*, ATLAS Note PHYS-NO-033 (1994).
- [65] D. Fouchez, ATLAS internal note PHYS-NO-160 (1994)
- [66] H. Aihara *et al.*, *FERMILAB-Pub-95/031*.
- [67] K. Hagiwara, S. Ishihara, R. Szalapski, and D. Zeppenfeld, *Phys. Lett.* **B283**, 353 (1992), *Phys. Rev.* **D48**, 2182 (1992).
- [68] J.R. Smith, CMS TN/95-179 (1995).
- [69] R. Casalbouni, *et al.*, *Int. J. Mod. Phys.* **A4**, 1065 (1989).
- [70] F. Abe, *et al.*, *Phys. Rev. Lett.* **74**, 2900 (1995), *Phys. Rev.* **D51**, 949 (1995).
- [71] A. Henriquez and L. Poggioli, ATLAS Note PHYS-NO-010 (1992).
- [72] D. Cavalli, *et al.*, ATLAS internal note PHYS-NO-053 (1994).
- [73] R. Kinnunen, D. Denegri and J. Tuominiemi, CMS-TN/94-233 (1994).